

https://dspace.org/

Modelling the dispersion of airborne pollutants in the Pretoria urban area

Zib, Pavel

2014-08-18
http://hdl.handle.net/10539/15199

Downloaded from a DSpace repository. https://dspace.org/

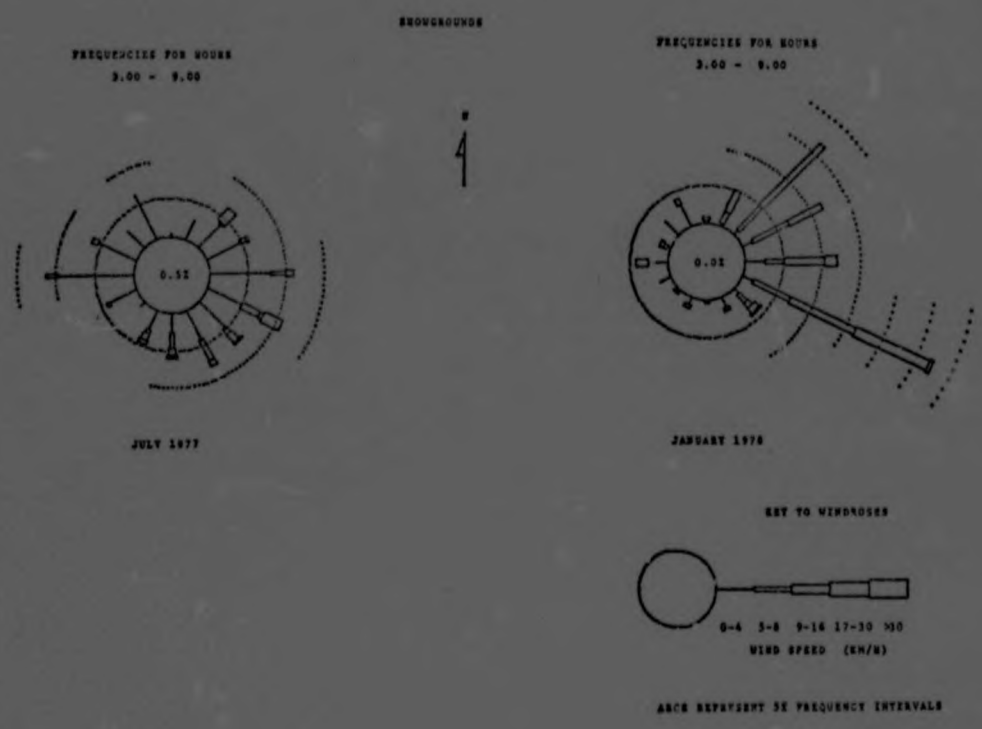


Figure 4.3 Windroses for the time interval 03h00 - 09h00 recorded during July 1977 and January 1978 at site No.2 in Pretoria

night and early morning contributes to the general decrease in the formation of surface-based inversions in summer.

4.1.3.2 Emission data

Winter, summer and annual emission rates of sulphur dioxide have been estimated from consumption figures using the emission factors for different types of fuel in Table 4.1. The emission factors express the amount of sulphur dioxide produced by burning a unit mass of fuel. Estimates of SO_2 emissions from industrial processes and in applications where control equipment has been installed, have been obtained directly from the industries concerned.

The location of individual sources has been specified using a rectangular grid array to overlay the modelled area. The origin (0;0) of the coordinate system in the lower lefthand corner in Figure 4.4 has the latitude of 20°53'27" south and the longitude of 27°51'08" east, with the x-axis pointing east and the y-axis pointing north. One grid unit represents 100 metres.

Table 4.1 Emission factors for estimating combustion related emissions of sulphur dioxide in Pretoria (sulphur and ash contents as quoted Bulletin 78, S.A. Fuel Research Institute, 1973)

Type of fuel	Sulphur content (%)	Ash content (%)	Emission factors
Coal	1,0	14,9	$1,9 \times 10^{-2}$
Anthracite	1,0	11,7	$1,9 \times 10^{-2}$
Coke	1,0	20,6	$1,9 \times 10^{-2}$
Heavy oil	3,4	-	$6,5 \times 10^{-2}$
Light oil	1,3	-	$8,5 \times 10^{-3}$
Paraffin	0,1	-	$1,7 \times 10^{-3}$
Gas	-	-	0
Wood	-	-	$7,5 \times 10^{-4}$

4.1.3.3 Wind and stability data

Mean hourly values of wind speed and wind direction have been determined from continuous records obtained at the centrally situated station No.1 during the period from October 1976 to November 1977. The hourly wind data have been distributed into sixteen wind sectors of a constant width and five wind speed classes. An example of the data is shown in Appendix C. Table 4.2 shows the range of wind speed and the central values for each class. The lowest class includes periods of near calm conditions during which the record has become indistinct as the result of a limited sensitivity of the instrument to very low wind speeds. The simple power law is invoked in the model to approximate the variation of wind speed with height (Table 3.3).

Table 4.2 Classification of wind speed in Pretoria

Wind speed class	Speed interval (m/sec)	Central speed (m/sec)
1	<1,11	1,0
2	1,39 - 2,22	1,8
3	2,50 - 4,45	3,5
4	4,72 - 8,34	6,5
5	>8,34	10,0

Note: By using the local Weather Bureau data, the wind classification for Pretoria does not exactly agree with the Pasquill classification of wind speed. This discrepancy is reconciled later in the modified scheme for estimating the stability categories in Table 4.3.

The division into Pasquill stability categories has been adopted and hourly estimates of stability conditions have been based on observations of the mean wind speed, on the season of the year and the time of the day using the scheme in Table 4.3. During the daytime the amount of incoming radiation is usually high irrespective of the season. Convective processes dominate in the planetary boundary layer and unstable

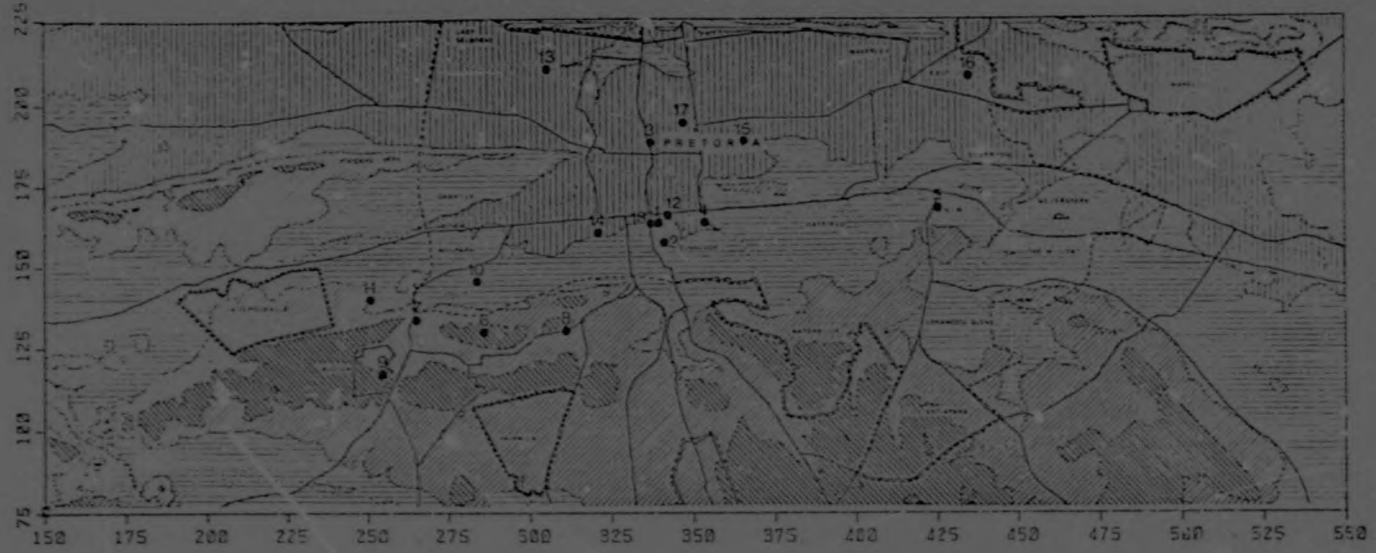




Figure 4.4 The coordinate system for locating emission sources in Pretoria. The circles indicate the position of SO_2 monitoring sites during 1977

conditi ns are established. The degr of atmospheric instability is then controlled in Table 4.3 by the mean wind speed. Low wind conditions will not significantly affect the convective process, whereas high wind speeds will reduce the extent of vertical motions.

At night inversions develop at the surface especi v under low wind conditions and clear skies. The incidence of well-developed surface-based inversions in Pretoria reaches a frequency of 80-90 percent in winter, 60-70 percent in autumn, 50-60 percent in spring and 40-50 percent in summer (Tyson et al., 1976). The intensity of the inversion is highest in winter and lowest in summer. Hence, the degree of atmospheric stability during nighttime conditions is determined in Table 4.3 by the season and the mean wind speed observed.

Table 4.3 The scheme for estimating Pasquill stability categories in Pretoria

Surface wind speed class	DAY	NIGHT		
	All seasons	Winter	Spring/Autumn	Summer
1	A	F	E	D
2	A	F	E	D
3	B	E	D	C
4	C	D	C	C
5	C	D	C	C

The mean duration of daytime and nighttime conditions has been estimated using acoustic sounder observations of the diurnal variation of static stability in the first 500 to 1000 metres of the atmosphere (von Gogh and Zib, 1978). Two monostatic acoustic sounders have been operated to monitor the continuous deve-

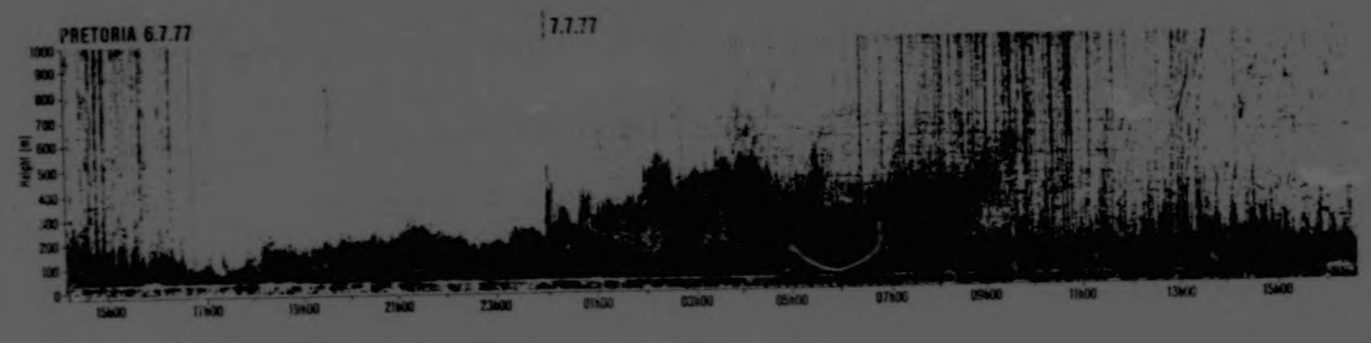


Figure 4.5 Acoustic sounder record showing the diurnal variation of the stability structure of the atmosphere over Pretoria in winter

lopment and decay of layers of positive and negative temperature gradients. The sounder facsimile record in Figure 4.5 has been obtained on 6-7 July, 1977 and illustrates the typical diurnal variation of the atmospheric structure over Pretoria in winter.

The decrease in the convective thermal activity in the afternoon of 6 July, 1977 was followed by a brief transitional period at about 17h30 during which virtually no echo pattern was recorded. A surface-based inversion developed soon after 18h00 and reached a depth of 200 metres by 22h00. Soon after midnight on 7 July, 1977 the further growth of the inversion was followed by separation of an elevated inversion. By 05h00 the two inversions merged again giving rise to a continuous surface inversion 400 metres deep. Lifting of the inversion began at 08h00 and the daytime echo pattern was fully established by 11h00. At the peak of the convective activity between 13h00 and 14h00 the thermals reached a depth of about 350 metres. The 24-hour cycle is closed by a gradual decrease in the afternoon instability towards the transition to evening stability.

Based upon records at different sites, daytime conditions have been taken to extend from 09h00 to 15h00 in winter, 09h00 to 18h00 in spring and autumn and 06h00 to 18h00 in summer. Three-hourly intervals (00h00 to 03h00, 03h00 to 06h00 etc.) corresponding to the time resolution of wind data analysis have been used for the division.

Finally, the monthly composite frequency functions $f(i,j,k)$ have been determined as the frequency of hourly occurence of the wind speed j within the sector i and the stability category k. Frequency functions for longer intervals have been obtained by integrating the monthly frequencies.

4.1.3.4 Dispersion parameters

The standard deviations $\sigma_z(x)$ have been determined using the division into x stability categories over hourly intervals. The

set of Pasquill curves have been approximated by the power law $\sigma_z(x) = cx^d$ for three ranges of downwind distance from the source. The values of the parameters c and d are shown in Table 4.4 for x_1 = 100 to 500 metres, x_2 = 500 to 5 000 metres and x_3 = 5 000 to 50 000 metres.

4.1.3.5 Plume rise

The effective height of all point sources has been estimated using the Briggs' (1969) formula for plume rise as

$$H = h + \frac{1,6\ F^{1/3}\ x^{2/3}}{u} \qquad (4.13)$$

for all stability categories. The calculation of the plume rise has been terminated at the distance downwind where the ratio $(x/14\ F^{5/8})$ has reached the limiting value of 3,5. The numerical value of the buoyancy term F is determined for each source from the stack dimensions and the physical parameters of the effluent. The validity of Equation (4.13) for describing the plume rise under atmospheric conditions found over Pretoria has been documented by Venter (1976).

4.1.3.6 Mixing height

The systematic variation of the mixing height with the season and the time of the day has been included in the model by introducing daytime and nighttime mean values. The mean values have been determined using the results of a recent survey on inversion climatology over South Africa (Tyson et al., 1976, Preston-Whyte et al., 1977). In winter the mean base of the elevated stable layer over Pretoria is situated about 1 750 metres above the ground. The corresponding elevation in summer is 2 090 metres. The height of 1 500 metres which represents the mean lower 90 % confidence level for all seasons has been selected the daytime mixing height. The value of 500 metres has been chosen to represent the mean nocturnal mixing height. A conservative value has been taken in order to minimize a possible error in dispersion estimates which is

Table 4.4 Values of dispersion parameters c and d in the Gaussian plume model (after Busse and Zimmerman, 1973)

Pasquill stability category	Downwind distance (metres)					
	x_1		x_2		x_3	
	c	d	c	d	c	d
A	0,0383	1,2812	0,0003	2,0886	-	-
B	0,1393	0,9467	0,0494	1,1137	-	-
C	0,1120	0,9100	0,1014	0,9260	0,1154	0,9109
D	0,0856	0,8650	0,2591	0,6869	0,7368	0,5642
E	0,0618	0,8155	0,2527	0,6341	1,2969	0,4421
F	0,0545	0,8124	0,2017	0,6020	1,5763	0,3606

known to have occurred when an unrealistically high value has been used. The frequency of occurence of elevated inversions with the base situated below 500 metres is given by Preston-Whyte et al. (1977) as 5% in winter and 10% in summer.

4.1.3.7 Removal rates of sulphur dioxide

No information concerning the removal rates of sulphur dioxide over Pretoria is available. Giebel (1977) suggests a total removal rate of 12,4% per hour for use in European conditions. Eliassen and Saltbones (1975) report a removal rate of slightly less than 10% per hour obtained from an experiment over long distances. The rate at which sulphur dioxide is depleted in the air over Pretoria has been taken as 10% per hour.

4.1.4 The presentation of results

A series of computer simulations covering the period from October 1976 to November 1977 has been carried out to obtain the estimates of ground-level concentrations. Mean monthly, three- and six-monthly and annual concentrations have been determined at regularly spaced receptor points. The spatial resolution of the estimated concentration field has been restricted by the available computer time. As the increase in the number of receptor points results in an almost linear increase in the computer time, the spacing between receptor points has been limited to 2 000 metres (20 grid units). Maps of concentration isopleths have been drawn using a rectangular array of receptor points.

Figures 4.6 to 4.8 show the winter, spring and annual concentration maps for 1977 predicted by the Gaussian plume model. The areas of high pollution levels during the respective seasons are clearly reflected in the predicted maps. Beginning in the west, an area of increased pollution corresponds to the high-density Black residential area of Atteridgeville. The pollution levels increase further east reaching the peak concentration in the highly industrialized part of metropolitan Pretoria. The gradual decrease in the influence of the industrial zone on the pollution

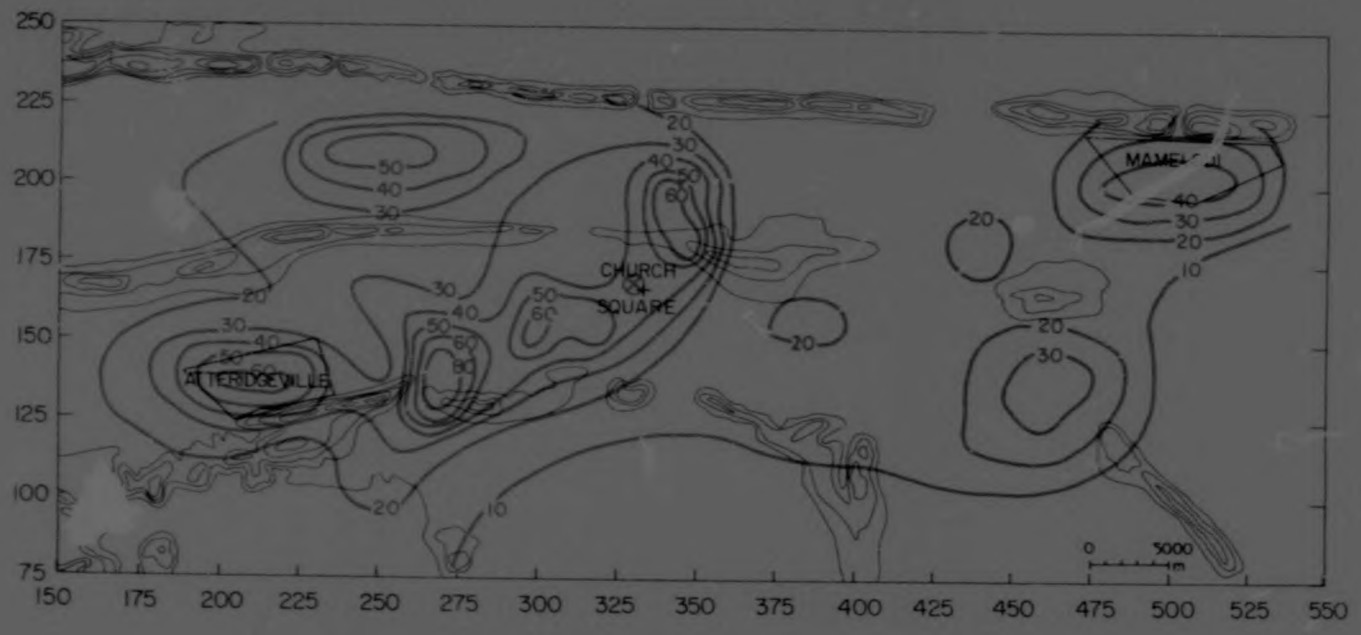


Figure 4.6 Isopleths of SO_2 concentration ($\mu g/m^3$) estimated for winter 1977 in Pretoria by the Gaussian plume model. The cross symbol indicates the station at which wind data have been recorded for the simulation

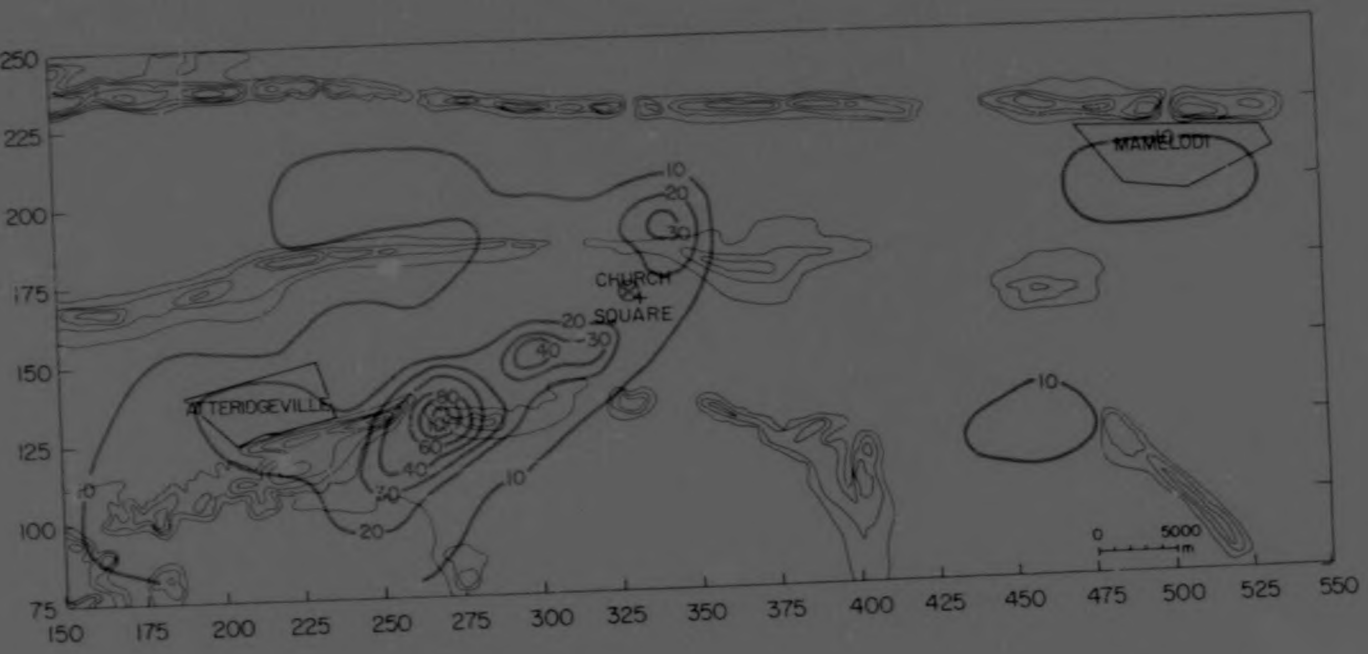


Figure 4.7 Isopleths of SO_2 concentration ($\mu g/m^3$) estimated for spring 1977 in Pretoria by the Gaussian plume model

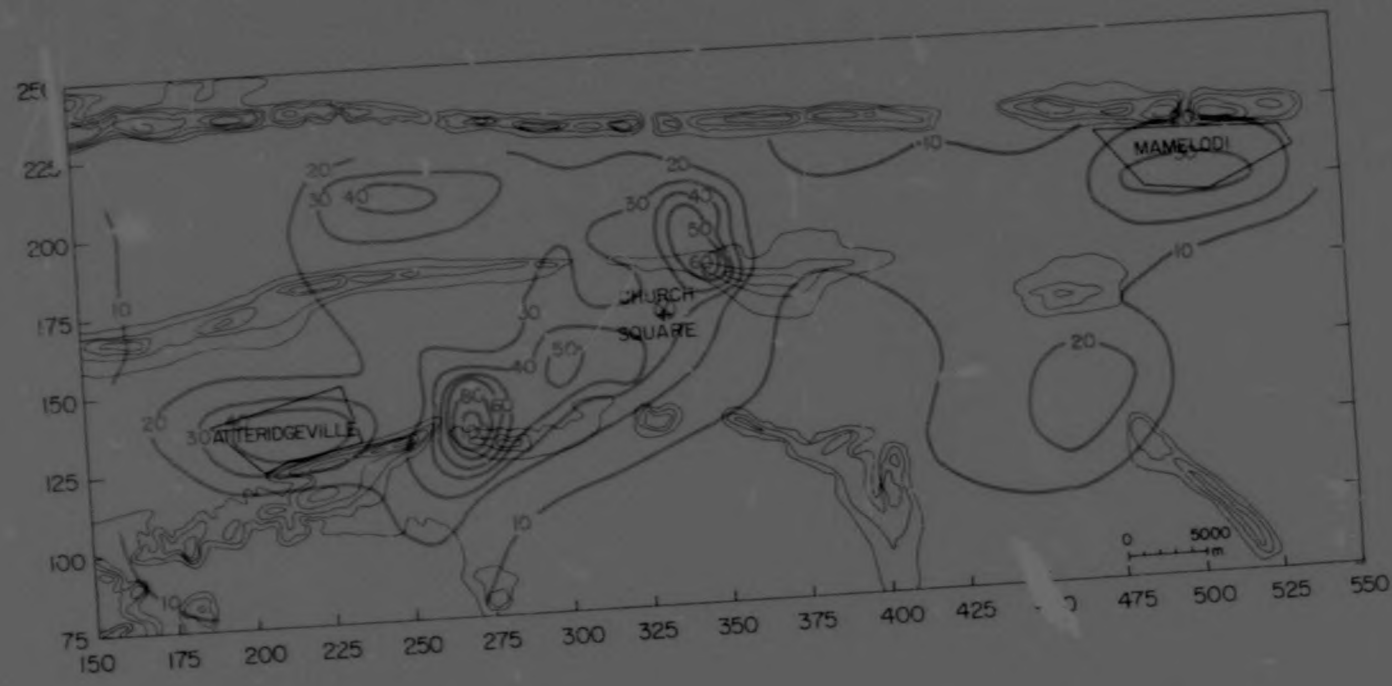


Figure 4.8 Isopleths of annual SO_2 concentration ($\mu g/m^3$) estimated for 1977 in Pretoria by the Gaussian plume model

towards the east is replaced by an increase in the influence of the commercial and business activities in the central business district, especially in winter. Generally low pollution levels are found over the suburban residential area to the east of the city centre. In accord with the estimated increase of SO_2 levels over Atteridgeville in the west, a similar pattern is established in the extreme east where another Black residential area is situated.

4.1.5 The analysis of results

Observed SO_2 concentrations which may be used to evaluate the performance of the model in Pretoria are available at a number of sites over various periods of time. Table 4.5 shows the location of monitoring stations and the duration of the record at each site. Table 4.6 shows a comparison of the estimates by the Gaussian plume model and the observed concentration levels for time intervals from one month to one year.

The model predictions are generally below the observed levels for all time intervals as indicated by the relative deviation given next to each pair of data. The relative deviation is defined as the deviation of the predicted concentration X from the observed value Y using the relationship

$$D = \frac{X-Y}{Y} \qquad (4.14)$$

The maximum negative deviation of - 0,68 occurred at stations 4 and 8 during November 1977. Station 4 is situated in a high-density residential area near the city centre whereas station 8 is on a ridge to the south-east of a major industrial complex. Lower values than those observed have been estimated at these stations throughout the year. In contrast, consistently higher estimates have been obtained at sites situated close to heavily polluting areas (stations 3, 7 and 9). Station 3 is located near a railway yard and stations 7 and 9 are in the industrial area west of the central district.

The degree of correlation between predictions and observations

Table 4.5 The location of SO_2 monitoring stations in Pretoria and the duration of the record at each site. The coordinates refer to the position on the grid in Figure 4.4

Identification number	Grid position		Identification	Duration of record
	X-coordinate	Y-coordinate		
1	335	163	Church Square	October 1976
2	341	157	Visagie Street	to
3	335	188	Myburgh Street	December 1977
4	354	162	Arcadia	
5	426	167	CSIR	
6	286	129	Iscor Dog School	June 1977
7	265	133	Iscor Hospital	to
8	311	130	Iscor Headquarters	November 1977
9	254	117	Lautium	
10	284	145	Iscor Training Centre	
11	250	132	SAP Dog School	
12	341	165	Munitoria	
13	305	210	Mountain View	
14	320	180	Iscor Club	July 1977
15	365	188	HF Verwoerd High School	
16	434	208	East Lynne	
17	346	194	Capital Park	
18	336	163	Church Square	

Table 4.6 Comparison of observed and predicted values of SO_2 concentrations ($\mu g/m^3$) by the Gaussian plume model in Pretoria

Station number and grid position	1 Month (July 1977)			1 Month (November 1977)			3 Months (Winter 1977)			3 Months (Spring 1977)			6 Months (June-Nov 1977)			12 Months (Oct 1976-Nov 1977)		
	Obs.	Pred.	Rel. dev.	Obs.	Pred.	Rel. dev.	Obs.	Pred.	Rel. dev.	Obs.	Pred.	Rel. dev.	Obs.	Pred.	Rel. dev.	Obs.	Pred.	Rel. dev.
1 (335;163)	62	58	-0,06	24	10	-0,58	59	55	-0,07	28	16	-0,43	43	30	-0,30	30	29	-0,03
2 (341;157)	52	32	-0,38	14	8	-0,43	47	31	-0,34	18	12	-0,33	31	20	-0,.[illegible]	24	19	-0,21
3 (335;188)	38	39	+0,03	12	16	+0,33	34	39	+0,15	19	28	+0,47	26	33	+0,27	16	32	+1,00
4 (354;162)	39	20	-0,49	22	7	-0,68	36	21	-0,42	20	10	-0,50	28	15	-0,46	20	15	-0,25
5 (426;167)	22	16	-0,27	9	3	-0,67	18	17	-0,06	11	7	-0,36	14	11	-0,21	10	11	+0,10
6 (286;129)	31	30	-0,03	32	29	-0,09	46	31	-0,14	30	30	0,00	33	30	-0,09			
7 (265;133)	74	77	+0,04	38	52	+0,37	62	81	+0,25	31	86	+1,77	48	83	+0,73			
8 (311;130)	38	25	-0,34	25	8	-0,68	36	24	-0,33	25	12	-0,52	28	18	-0,36			
9 (254;117)	34	39	+0,15	28	31	+0,11	29	32	+0,10	27	42	+0,56	35	37	+0,06			
Correlation coefficient	0,88			0,80			0,86			0,63			0,77					
Mean rel. deviation	-0,15			-0,26			-0,09			+0,07			-0,08					
Standard error	9,9 $\mu g/m^3$			10,40 $\mu g/m^3$			10,60 $\mu g/m^3$			20,80 $\mu g/m^3$			14,50 $\mu g/m^3$					

has been ascertained in Table 4.6 by the correlation coefficient defined as (Brooks and Carruthers, 1953)

$$R_{x,y} = \frac{\left[N\sum_{i=1}^{N}(X_i Y_i)\right] - \left[\left(\sum_{i=1}^{N}X_i\right)\left(\sum_{i=1}^{N}Y_i\right)\right]}{\left\{\left[N\sum_{i=1}^{N}X_i^2 - \left(\sum_{i=1}^{N}X_i\right)^2\right]\left[N\sum_{i=1}^{N}Y_i^2 - \left(\sum_{i=1}^{N}Y_i\right)^2\right]\right\}^{\frac{1}{2}}} \qquad (4.15)$$

The correlation coefficient ranges from 0,63 during the spring to 0,88 in July. In the case of a systematic overprediction or underprediction by the model the degree of association as expressed by the correlation coefficient may remain relatively high. In order to obtain an indication of the sign and the magnitude of the deviations two additional indicators of the model performance have been used in Table 4.6. They include the mean relative deviation

$$\bar{D}_{x,y} = \frac{1}{N}\sum_{i=1}^{N}\left(\frac{X_i - Y_i}{Y_i}\right) \qquad (4.16)$$

and the standard error of estimate

$$\hat{S}_{y,x} = \left\{\frac{1}{N}\left[N\sum_{i=1}^{N}Y_i^2 - \left(\sum_{i=1}^{N}Y_i\right)^2\right] - \frac{\left[N\sum_{i=1}^{N}X_i Y_i - \sum_{i=1}^{N}X_i\sum_{i=1}^{N}Y_i\right]^2}{\left[N\sum_{i=1}^{N}X_i^2 - \left(\sum_{i=1}^{N}X_i\right)^2\right]}\right\}^{\frac{1}{2}} \qquad (4.17)$$

The only time interval (spring 1977) during which the mean concentration levels have been overestimated is also associated with the maximum standard error of estimate of 20,8 $\mu g/m^3$. The full range of the standard error of estimate is from 9,9 $\mu g/m^3$ (July 1977) to 20,8 $\mu g/m^3$ (spring 1977). The lowest and highest deviations are + 0,07 (spring 1977) and - 0,26 (November 1977) respectively.

4.2 The application of the ATDL-grid model

In the ATDL-grid model Gaussian description of concentration distribution is retained and the dependence on the crosswind dispersion removed by considering only emissions situated in a narrow upwind sector. A grid system in Figure 4.9 is used to divide Pretoria into a regular array of horizontal squares over which the area source strength is defined. The grid squares also serve as receptor squares in that the concentration in each square is determined as the spatial average from contributions by point and area sources.

4.2.1 Point sources

The contribution of large elevated sources to the long-term concentration in a ground-level receptor square is calculated as

$$\bar{\chi} = \left(\frac{2}{\pi}\right)^{\frac{1}{2}} \left(\frac{n}{2\pi}\right) \frac{Q \cdot f}{r\, u\, \sigma_z} \exp\left(-\frac{H^2}{2\sigma_z^2}\right) \qquad (4.18)$$

The frequency function f describes the distribution of wind direction among n sectors in respect to a fixed receptor. A constant wind speed u is defined for the entire urban area. The symbol r denotes the distance between the centres of the respective grid squares in which the source and the receptor are located.

4.2.2 Area sources

The lesser emissions are grouped in grid squares of 500 × 500 metres into area sources which are assumed to emit pollutants at the ground level. The Gaussian dispersion formula for a ground-level area source may be derived from Equation (4.1). by setting H=0 as

$$\bar{\chi}\ (x,y,0,0) = \frac{Q}{\pi\, u\, \sigma_y\, \sigma_z} \exp - \left(\frac{y^2}{2\sigma_y^2}\right) \qquad (4.19)$$

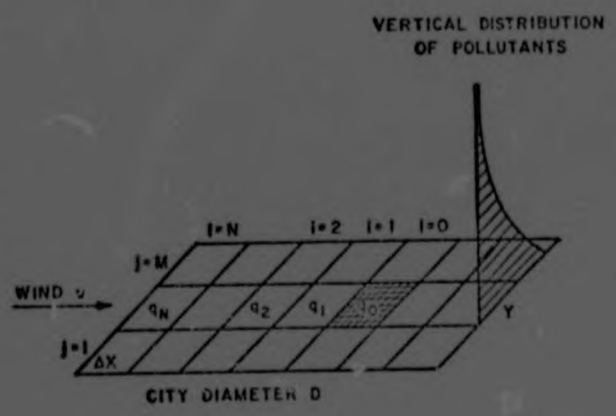


Figure 4.9 The concept of the ATDL-grid model. The concentration is calculated in the centre of each grid square assuming Gaussian vertical distribution

and by integrating Equation (4.19) with respect to y from $-\infty$ to ∞ and with respect to x from 0 to ∞. Hence, the concentration from an area source situated in the upwind plane from the receptor square is given by

$$\bar{\chi} = \int_{0}^{\infty}\int_{-\infty}^{\infty} \frac{Q(x,y)}{\pi u \sigma_y(x)\sigma_z(x)} \exp - \left[\frac{y^2}{2\sigma_y^2(x)}\right] dy\, dx \qquad (4.20)$$

The first integration yields

$$\bar{\chi} = \left(\frac{2}{\pi}\right)^{\frac{1}{2}} \int_{0}^{\infty} \frac{Q(x)}{u\,\sigma_z(x)} dx \qquad (4.21)$$

If the source strength Q(x) does not change significantly with the position x within the grid squares, a constant source strength q_i may be introduced in each square, where

$$\sum_{i=1}^{N} q_i = \int_{0}^{\infty} Q(x)\, dx \qquad (4.22)$$

and N is the number of upwind grid squares (Figure 4.9). It has been shown by Gifford and Hanna (1970) that the solution of Equation (4.21) for the simple power-law form of the dispersion parameter $\sigma_z(x) = ax^b$ may be written as

$$\bar{\chi} = \left(\frac{2}{\pi}\right)^{\frac{1}{2}} \frac{1}{u\,a\,(1-b)} \left(\frac{\Delta x}{2}\right)^{1-b} \left[q_o + \sum_{i=1}^{N} f_i\, q_i \left[(2i+1)^{1-b} - (2i-1)^{1-b}\right]\right] \qquad (4.23)$$

Equation (4.23) has been generali. . by including the frequency distribution of wind direction for the long-term application.

In order to limit the execution time of the program the calculation at a grid centre has been terminated when four neighbouring area sources in each direction had been scanned and their contribution to the total concentration determined. In contrast, the plumes from the point sources have been allowed to travel to

any location within the modelled area and to contribute to the concentration at even the most distant receptors. Although this provision increases the execution time by more than a factor of two, a restriction similar to that imposed on the travel of plumes from area sources would introduce a significant error, particularly in estimates at distant receptors in stable conditions.

4.2.3 Input data

The emission data have been regrouped to suit the spatial requirements of the model. In each grid square a constant source strength has been determined and the point sources have been assigned to the square centres. The mean wind speed, the frequency distribution of directional occurence for each of 16 wind sectors and the mean stability conditions have been determined on a monthly basis. Standard deviations σ_z have been assigned numerical values from the scheme in Table 4.7, based on dispersion parameters given by Smith (1968) and extended by Gifford and Hanna (1970). The simple power law $\sigma_z = ax^b$ has been used to approximate the variation of σ_z with downwind distance x.

Table 4.7 Values of dispersion parameters a and b in the ATDL-grid model (after Gifford and Hanna, 1970)

Mean stability conditions	Estimated Pasquill category	a	b
Very unstable	A	0,40	0,91
Unstable	B	0,33	0,86
Neutral	C	0,22	0,80
Estimated urban	D	0,15	0,75
Stable	E,F	0,06	0,71

4.2.4 The presentation and analysis of results

Isopleths of winter, spring and annual SO_2 concentrations in Figures 4.10 to 4.12 predicted by the ATDL-grid model have been drawn using the centre-point values in each receptor square. Although the spatial distribution of the estimated high SO_2 levels corresponds to the position of the main polluting areas in Pretoria the estimated values are high, especially during the winter season.

Table 4.8 shows that the estimated winter concentrations in or near the central business district (Stations 1 to 4) exceed significantly the available observations. The maximum relative deviation reaches a high value of +4,26 at Church Square (Station 1) in July 1977. A slight overestimation is also obtained at the industrial sites (Stations 7 to 9) whereas the winter estimates at the lightly polluted stations 5 and 6 are somewhat below the observed levels. The mean relative deviations of +1,72 in July 1977 and +1,50 for the whole winter season reflect the strong overestimation at the central sites. The values of the standard error are also high (91,5 $\mu g/m^3$ in July and 81,6 $\mu g/m^3$ in winter) and the correlation coefficients low (0,57 and 0,55 respectively).

The significant overprediction at the central sites is absent during the spring season and the estimates agree more closely with observations. A mean relative deviation of -0,05 and a standard error of 8,9 $\mu g/m^3$ have been recorded in November 1977. The corresponding values for the spring season are -0,02 and 8, $\mu g/m^3$. The correlation coefficients have also increased to 0,64 in November and 0,72 in spring. However, the semi-annual and to a lesser degree the annual predictions are affected by the high winter values at the central sites.

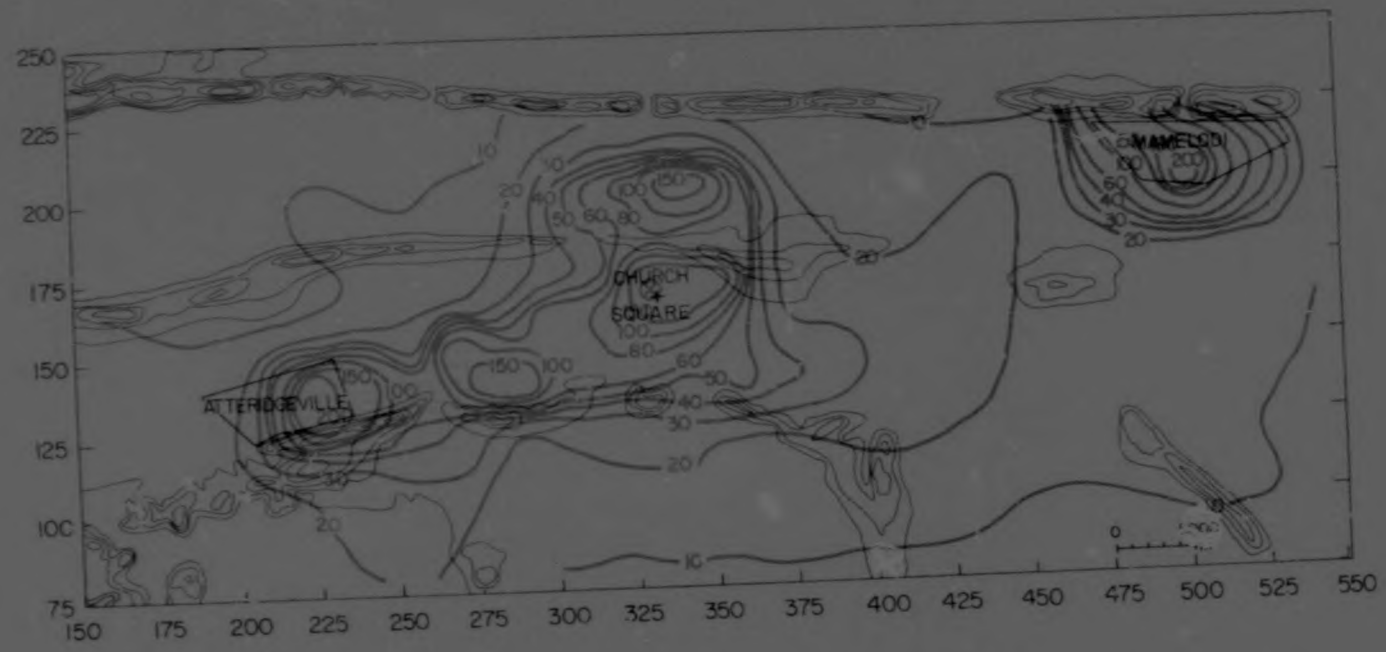


Figure 4.10 Isopleths of SO_2 concentration ($\mu g/m^3$) estimated for winter 1977 in Pretoria by the ATDL-grid model. The cross symbol indicates the station at which wind data have been recorded for the simulation

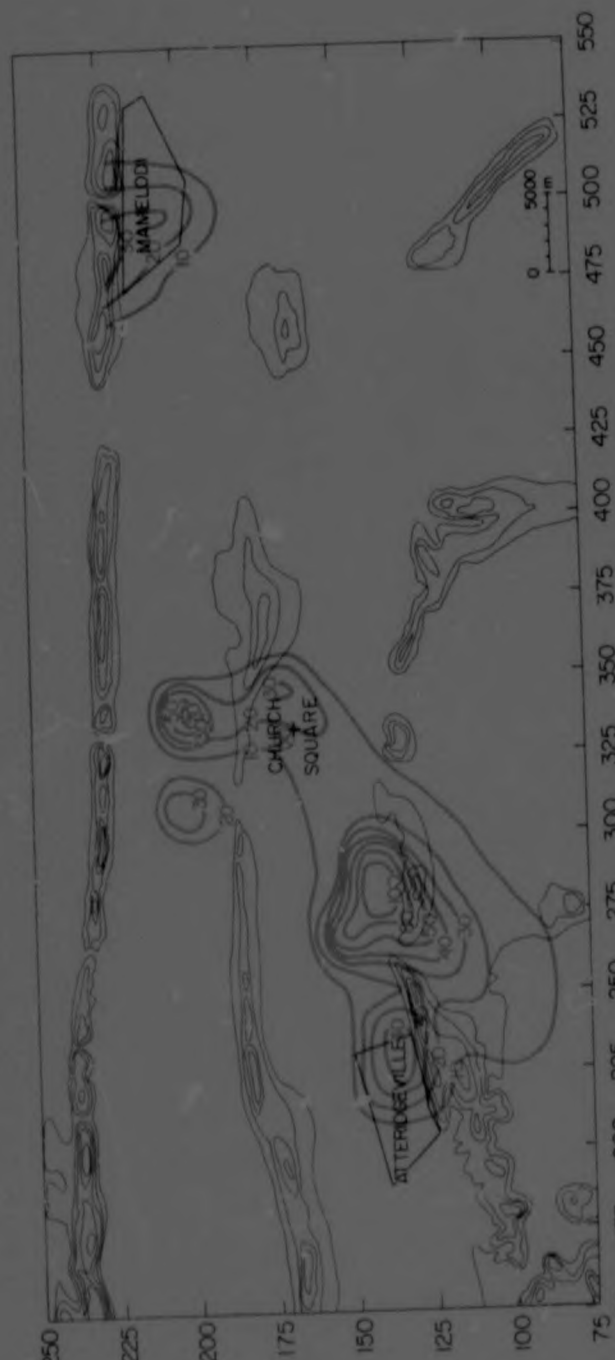


Figure 4.11 Isopleths of SO_2 concentration ($\mu g/m^3$) estimated for spring 19/7 in Pretoria by the ATDL-grid model

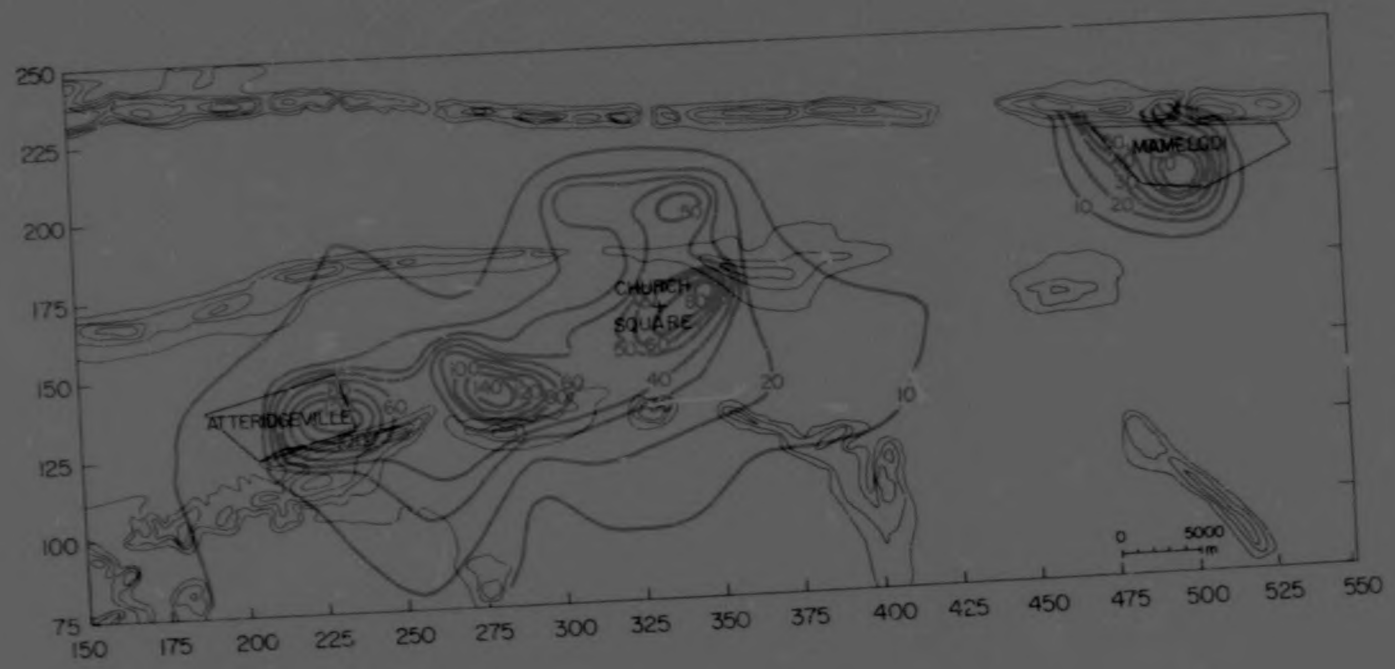


Figure 4.12 Isopleths of annual SO_2 concentration ($\mu g/m^3$) estimated for 1977 in Pretoria by the ATDL-grid model

Table 4.8 Comparison of observed and predicted values of SO_2 concentrations ($\mu g/m^3$) by the ATDL-grid model in Pretoria

Station number and grid position	1 Month (July 1977)			1 Month (November 1977)			3 Months (Winter 1977)			3 Months (Spring 1977)			6 Months (June-Nov 1977)			12 Months (Oct 1976-Sept 1977)		
	Obs.	Pred.	Rel. dev.	Obs.	Pred.	Rel. dev.	Obs.	Pred.	Rel. dev.	Obs.	Pred.	Rel. dev.	Obs.	Pred.	Rel. dev.	Obs.	Pred.	Rel. dev.
1 (335;163)	62	326	+4,26	24	20	-0,17	59	283	+3,80	28	22	-0,21	43	63	+0,47	30	78	+1,60
2 (341;157)	52	237	+3,56	14	28	+1,00	47	199	+3,23	18	30	+0,67	31	78	+1,52	24	97	+3,00
3 (335;188	38	130	+2,58	12	13	+0,08	34	126	+2,71	19	17	-0,11	26	45	+0,73	16	52	+2,25
4 [illegible]4;162)	39	179	+3,59	22	22	0,00	36	156	+3,33	20	24	+0,20	28	55	+0,96	20	67	+2,35
5 ([illegible];167)	22	20	-0,09	9	2	-0,78	18	17	-0,06	11	2	-0,82	14	6	-0,57	10	8	-0,20
6 (286;129)	31	22	-0,29	32	39	+0,22	36	21	-0,42	30	40	+0,33	33	34	+0,03			
7 (265;133)	74	96	+0,16	38	25	-0,34	65	64	-0,02	31	33	+0,06	48	45	-0,06			
8 (311;130)	38	76	+1,00	25	13	-0,48	36	62	+0,72	25	13	-0,48	28	36	+0,29			
9 (254;117)	34	59	+0,74	28	29	+0,03	29	34	+0,17	27	32	+0,19	35	40	+0,14			
Correlation coefficient	0,57			0,64			0,55			0,72			0,52					
Mean rel. deviation	+1,72			-0,05			+1,50			-0,02			+0,39					
Standard error	91,5 $\mu g/m^3$			8,9 $\mu g/m^3$			81,6 $\mu g/m^3$			8,7 $\mu g/m^3$			18,4 $\mu g/m^3$					

4.3 The application of the Gifford-Hanna simple model

Several workers (Halliday and Venter,1971, Hanna, 1971, Gifford and Hanna, 1973) have pointed out that the production of the ground-level concentration in an urban area may often be approximated by the simple relationship

$$\bar{\chi} = C \frac{q}{u} \qquad (4.20)$$

in which the variations of dispersion conditions may be included in the factor of proportionality C. This relationship is used in the model to estimate the contribution from area sources to the total concentrations. The geometry of the grid model has been retained to define the size and the position of the sources.

4.3.1 Point sources

The point sources are treated in the model in a way which is identical to the treatment in the ATDL-grid model. It includes considerations of source elevation and the variation of wind direction.

4.3.2 Area sources

The manner in which Equation (4.20) may be incorporated into a dispersion model was postulated by Hanna (1971) using the concept of the ATDL-grid model. The Gifford-Hanna simple model rests on the assumption that the effect of remote sources on the concentration in the receptor square decreases rapidly with increasing distance and therefore, unless the source strengths q_i in the outside squares differ significantly from the source strength q_o in the receptor square itself, the equality $q_i = q_o$ may be introduced into Equation (4.19). Equation (4.19) becomes

$$\bar{X} = \left[\left(\frac{2}{\pi}\right)^{\frac{1}{2}} \frac{(N \cdot \Delta x)^{1-b} + \left(\frac{\Delta x}{2}\right)^{1-b}}{a\ (1-b)}\right] \frac{q_o}{u} \qquad (4.21)$$

expressing the concentration in the receptor square in proportion to the ratio between the emission rate q_o in the square and the wind speed u. The factor of proportionality includes considerations of atmospheric stability and the distance to the upwind edge of the city D and may be determined as

$$C = \left(\frac{2}{\pi}\right)^{\frac{1}{2}} \frac{D}{a\ (1-b)} \qquad (4.22)$$

4.3.3 Input data

The emission data have been converted into constant rates over the grid size of 2 000 × 2 000 metres. Neutral stability conditions for time scales of six and twelve months have been assumed for which a constant value of C = 50 has been adopted. Corresponding monthly wind speeds have been averaged to obtain semi-annual and annual mean values.

4.3.4 The presentation and analysis of results

The map of predicted concentration isopleths for the year 1977 is shown in Figure 4.13 and the degree of association between the predicted and observed pollution levels over six and twelve months in Table 4.9. Although the predictions at the central sites are still higher than the observed concentrations, a relative mean deviation of +0,23 is achieved and the standard error reduces to 8,8 $\mu g/m^3$ for the June - November 1977 interval. The corresponding correlation coefficient increases to 0,85.



Figure 4.13 Isopleths of annual SO_2 concentration ($\mu g/m^3$) estimated for 1977 in Pretoria by the Gifford-Hanna simple model

Table 4.9 Comparison of observed and predicted values of SO_2 concentrations ($\mu g/m^3$) by the Gifford-Hanna simple model in Pretoria

Station number and grid position	6 Months (June-Nov 1977)			12 Months (Oct 1976 - Sept 1977)		
	Obs.	Pred.	Rel. dev.	Obs.	Pred.	Rel. dev.
1 (335;163)	43	45	+0,05	30	54	+0,80
2 (341;157)	31	54	+0,74	24	69	+1,88
3 (335;188)	33	45	+0,06	16	47	+1,94
4 (354;162)	15	28	+0,87	20	34	+0,70
5 (426;167)	11	5	-0,55	10	7	-0,30
6 (286;129)	30	33	+0,10			
7 (265;133)	83	58	-0,30			
8 (3[illegible]1;130)	18	36	+1,00			
9 (254;117)	37	42	+0,14			
Correlation coefficient	0,85					
Mean rel. deviation	+0,23					
Standard error	8,8 $\mu g/m^3$					

CHAPTER 5

EVALUATION OF DISPERSION MODELS WITH APPLICATION TO PRETORIA

5.1 The evaluation of the Gaussian plume model for multiple sources

5.1.1 Performance and accuracy

When the degree of association between model predictions and the observed concentrations is used as a measure of the performance of individual models in Pretoria, the Gaussian plume model shows the best results. The magnitude of the highest mean deviation and of the maximum standard error together with the range of correlation coefficients indicate that the model realistically reflects the actual concentration distribution in Pretoria. The deviations of predictions from observations do not vary significantly with seasonally-induced changes in dispersion conditions and the model gives a balanced performance throughout the year. However, the occasionally higher deviations at individual receptors show that the sound overall performance of the model cannot be interpreted as a proof of its capacity to estimate pollution levels with the same degree of accuracy at all sites.

The assumption made in the model that the meteorological parameters measured at a single observation site are representative of the dispersion conditions in the whole of Pretoria is a gross simplification of reality. The interaction of the topographical and meteorological factors in Pretoria is known to cause marked local variations in the dispersion conditions (van Vuuren, 1978). The variations cannot be included in the present form of the Gaussian plume model.

A numerical experiment has been designed to examine the effect of this simplification on the concentration estimates. The original set of input data obtained at the Weather Bureau (site No.1) has

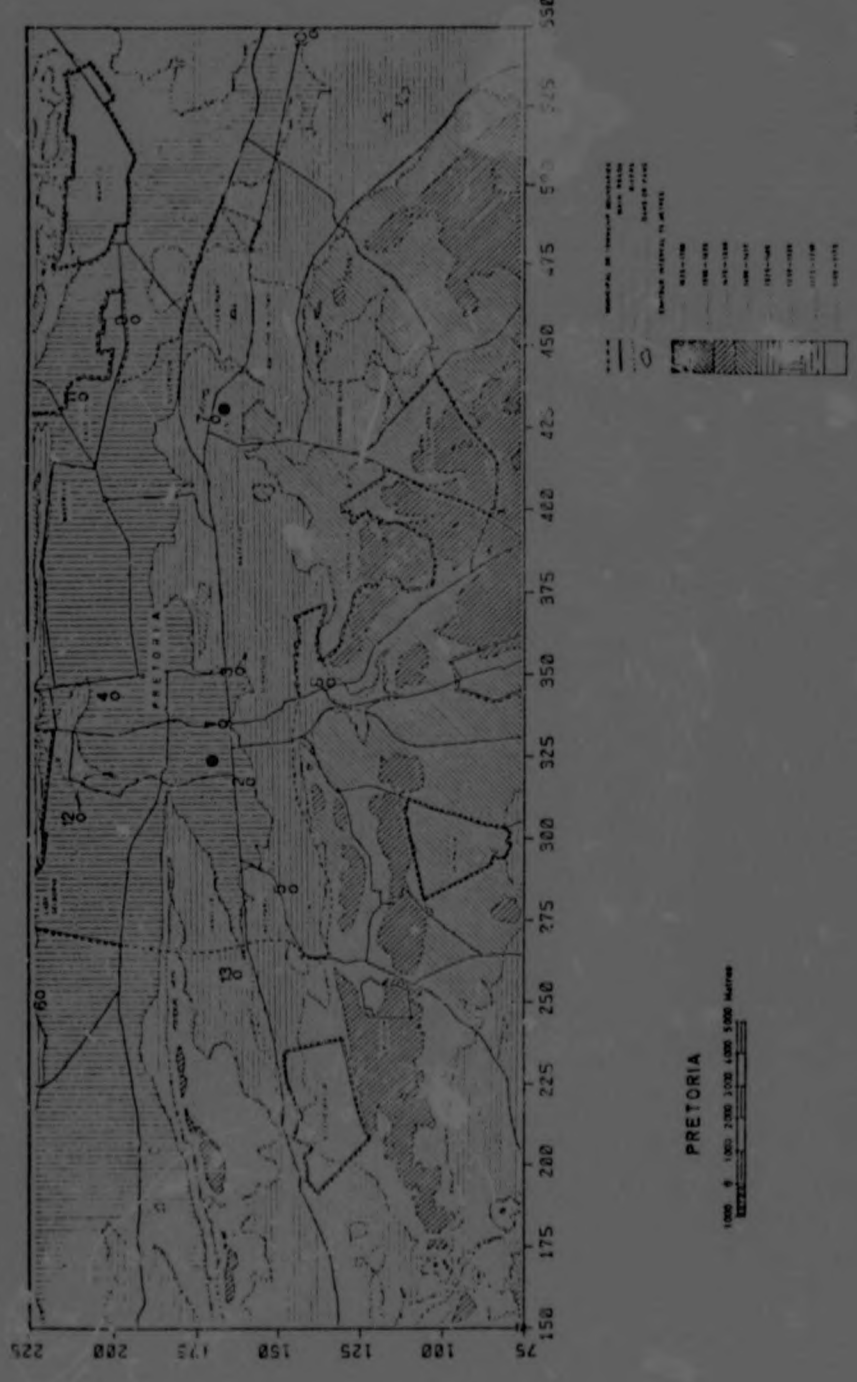


Figure 5.1 Location of wind recording stations in Pretoria during 1977.
Full circles indicate sites used for acoustic sounding

been replaced successively in the simulation by the meteorological data measured during 1977 at the sites in Figure 5.1. Winter SO_2 concentrations for 1977 have been simulated using the frequency of occurence of wind speed classes, stability categories and wind direction at each site at a time and related to observed concentrations in Table 5.1. The mean relative deviation from the observations ranges from -73,2 percent when the wind data from a rural site (site No.10) are used to +48,3 percent for a suburban site (site No.12) situated in the northern valley. For comparison, the mean relative deviation for the original site (site No.1) is -9,0 percent. The significant magnitude of the error associated with the

Table 5.1 Correlation between simulated and observed SO_2 concentrations in Pretoria during winter 1977 when meteorological conditions are individually represented in the Gaussian plume model by single-point measurements

Site of meteorological measurement		Mean rel. deviation	Standard deviation	Correlation coefficient
Number	Identification	(%)	($\mu g/m^3$)	
1	Forum Building	- 9,0	10,6	0,86
2	Showgrounds	- 4,5	8,3	0,96
3	Caledonian	-41,2	21,3	0,50
4	Capital Park	-49,0	11,1	0,80
5	Iscor	-25,0	12,6	0,88
6	Zandfontein	12,3	9,5	0,91
7	CSIR	-25,4	15,6	0,66
8	Fountains	-43,8	22,2	0,68
9	Siemens	-52,5	24,3	0,56
10	Hazeldene	-73,2	32,2	0,39
11	East Lynne	-41,2	21,2	0,51
12	Mountain View	48,3	36,6	0,26
13	Pretoria West	14,3	15,4	0,65

assumption of a spatially invariable wind and stability field in the model is further expressed by the range of standard deviations from 8,3 $\mu g/m^3$ to 36,6 $\mu g/m^3$ representing 20 to 90 percent of the mean winter concentration. The correlation coefficients vary with the location of the single-point measurements from 0,26 for the site No.10 to 0,91 for the site No.6. A subjective selection of the site at which meteorological observations are carried out thus becomes an important factor in the model.

5.1.2 Sensitivity analysis

In addition to being contingent on the ability of the model to simulate the real atmosphere, the accuracy of model predictions also depends on the accuracy of the input data. The degree to which errors and inaccuracies in the input are reflected in the model predictions is known to vary with the type of the input parameter. A sensitivity analysis may be performed (Hilst, 1970, Thayer and Koch, 1972) in order to investigate the responses of the model to changes in differing input parameters. The magnitude of the response is used to judge the degree of sensitivity of the model to variations in a specific parameter.

A large number of computer simulations have been carried out to examine the responses of the Gaussian plume model to systematic and random variations in the input data set for Prestonia. Systematic variations have been simulated by introducing incremental changes of -50 percent, -10 percent, +10 percent and +50 percent of the original input value into the data set. Concentration estimates have been obtained for these variations by the model at receptor points at regular intervals of 5000 metres. The magnitude of the model response has been expressed as the relative deviation of the predicted concentration from the originally estimated value x_o. The investigated parameters included the emission rate of sulphur dioxide, the height of the source, the wind speed, the standard deviation of pollutant distribution σ_z, the mixing height and the rate of SO_2 removal. Figure 5.2 shows the mean deviation for each input parameter. Whereas the concentration levels rise linearly with an overall increase in the emission rate, the response of the model to a longer residence period of sulphur dioxide in the atmosphere as expressed

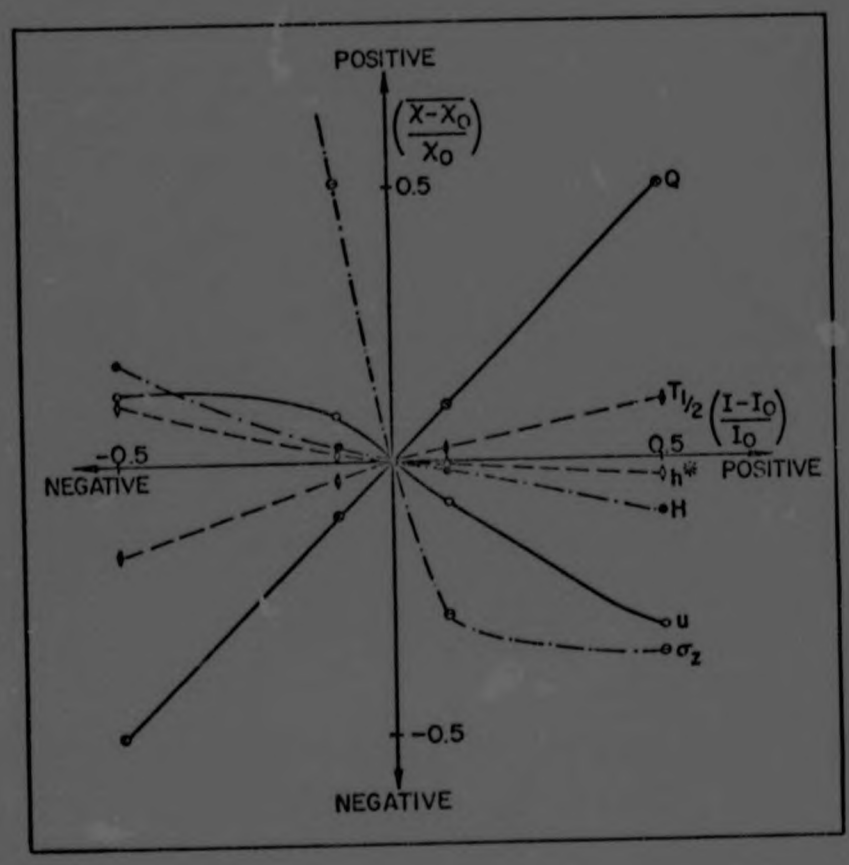


Figure 5.2 The mean deviation of concentration predictions $(\overline{\chi - \chi_o})/\chi_o$ in response to systematic variations of input parameters $(I - I_o)/I_o$

by the half-time constant is much weaker. An increase in the input value of the other four parameters results in an overall reduction of the predicted concentration levels. When the same rate of fractional change from the original value is introduced into the input, the variation of the vertical dispersion parameter σ_z results in the largest digression of the predicted SO_2 concentration from observations. The high sensitivity to a systematic variation of σ_z is followed in magnitude by the sensitivity to a variation of the central wind speed in each wind speed class, to changes in the emission height and in the mixing height.

Random variations have been simulated by randomly increasing or reducing an input value by 100 percent. No significant mean deviation in the estimated concentration levels has been found for either of the investigated input parameters.

In addition to the analysis of the sensitivity of the Gaussian plume model in individual input parameters, the sensitivity to possible errors in the composite frequency function f(i,j,k) has also been investigated. As in the case of individual parameters, random errors in the determination of the appropriate combination of wind speed classes, wind sector and stability category for each hourly interval do not result in significant deviations in the predicted concentrations. By contrast, Figure 5.3 shows the deviations obtained by introducing systematic errors into the frequency function. When the stability class is changed systematically by one category towards a more stable one (A → B, B → C, C → D, D → E, E → F, F), the mean deviation in the predicted concentration is +24 percent with individual deviations ranging from 0 to + 100 percent of the original concentration. A change towards a less stable category (F → E, E → D, D → C, C → B, B → A, A) produces a mean reduction of 8 percent and a narrower range of individual deviations. Similarly, a systematic underestimation of the wind speed class by one class (5 → 4, 4 → 3, 3 → 2, 2 → 1, 1) results in an increase of 12,5 percent in the concentration. The corresponding reduction for a positive error in the speed classification by one class (1 → 2, 2 → 3, 3 → 4, 4 → 5, 5) is -40 percent. In both cases the individual deviations range from 0 to 100 percent of the original concentration value. A systematic error by one sector in the determi-

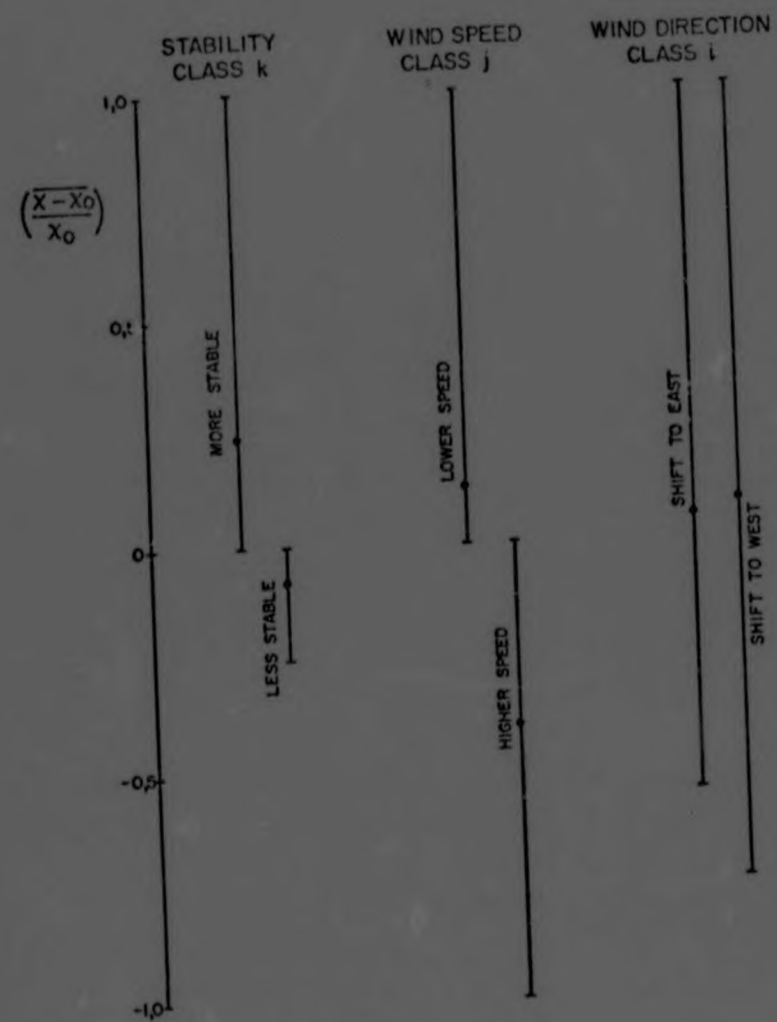


Figure 5.3 Deviations of concentration predictions $(\overline{X - X_0})/X_0$ in response to systematic errors in the composite frequency function f(i,j,k)

nation of the wind direction does not produce a significant mean deviation of prediction results. The range of individual deviations, on the other hand, is extremely wide from -70 percent to +100 percent for a shift of the wind direction by 22,5 de rees towards the west.

5.1.3 Discussion

The evaluation of the long-term Gaussian plume model has shown a good general performance of the model in Pretoria. The accuracy of predictions at individual sites is affected by the way in which the spatially variable wind and stability fields are treated in the model. The use of meteorological measurements from a single observation site is a very simplistic way to describe the complex wind and stability structure in an urban area. The structure varies in time and space and is compounded by the effects of topography and by variations in the surface roughness and the heat budget of a city. Hence, the ability of the Gaussian plume model to approximate the real state of the atmosphere and thus the concentration distribution of pollutants may further be improved by including considerations of spatially variable wind and stability fields in the model.

An additional source of error in the predictions are possible inaccuracies in the input data. The sensitivity analysis has shown that the model is most sensitive to systematic variations in the emission rate and in a variety of meteorological data. The critical meteorological parameters have been identified as the vertical dispersion parameter σ_z and the variables in the composite frequency function, i.e. the wind speed, wind direction and atmospheric stability. The model has been shown to be less sensitive to systematic variations in the emission height, the rate of removal of sulphur dioxide from the atmosphere and in the mixing height as well as to random errors in the input data set. The generally low sensitivity to random variations can be attributed to the smoothing effect of the large amount of data which are normally used in the multiple-source environment. The results of the sensitivity study imply that a random error in one of the critical input parameters will not cause a significant error in the overall performance of the model,

whe as a systematic error in the same parameter, even of a lesser magnitude, may result in a large error in the model predictions. The knowledge of critical input parameters as well as of the type of the error in the input data set which has a significant effect on the results of modelling applications can be utilized in the design of data acquisition and preparation programmes. As the resources available for the data collection are frequently limited, most of the experimental emphasis may be directed at the acquisition of the sensitive input data.

5.2. The evaluation of the ATDL-grid model

The model does not adequately describe the dispersion process in the complex Pretoria urban area. A significant overestimation is consistently found during the winter season and deviations of the factor of three to four from measured concentrations are common. The highest deviations occur at sites in or near the central business district where a large number of low-level sources are situated. By contrast to the winter situation, the predictions in the city centre are much closer to the observations in spring when the number of active low-level sources decreases substantially. The predictions for the industrial area to the west of the central business district where elevated point sources are the dominant factor in the emissions, are in a considerably better agreement with the measurements for all seasons.

During the winter most of the low-level sources are active when unfavourable dispersion conditions prevail associated with the development of strong surface-based inversions and low wind speeds. The inversions are most intense in a shallow layer immediately above the ground and the true physical height at which the effluent is released plays a vital role in the dispersion process. By contrast, the low-level sources are treated in the model as ground-based area sources. Hence, the assumption of effluent release from area sources at the ground must be seen as the major cause of the model's failure. The concept of defining a spatially invariable mean wind vector for the entire city and the absence of the removal term from the model equation also contribute to the reduced performance.

There is no way to include considerations of the real height of the low-level sources in the model while retaining the relative simplicity of the model equation for area sources. Hence, owing to its poor performance and little potential for refinement, the ATDL-grid model must be rejected as inadequate for the Pretoria situation.

5.3 The evaluation of the Gifford-Hanna simple model

In the Gifford-Hanna simple model the contribution from low-level sources is estimated in proportion to the ratio of the integrated emission rate in the grid square to the mean wind speed in the whole area. If the factor of proportionality C is determined empirically the discrepancy between the real emission height of the low-level sources and the concept of ground-based area sources in the model is eliminated. When a value of C = 50 is taken to represent the mean semi-annual and annual dispersion conditions in Pretoria, a much closer agreement with measured SO_2 concentrations is obtained than by the application of the ATDL-grid model. However, estimates of the concentration field are not possible to make over time intervals during which the mean dispersion conditions cannot be approximated by a neutral state of the atmosphere, for instance over a month or a season. The potential for refining the Gifford-Hanna simple model to include considerations of temporal variations in the concentration levels therefore rests in introducing dependence on atmospheric stability into the factor C.

PART III - MODEL REFINEMENTS

CHAPTER 6

REFINEMENTS OF URBAN AIR POLLUTION DISPERSION MODELS

The application to Pretoria has revealed the capabilities and the deficiencies of some of the mathematical models which are used for estimating the concentration levels of atmospheric pollutants in the city air. It has also indicated the potential for refinement of individual models and for improvement of their performance. In this chapter refinements to the Gifford-Hanna simple model and to the Gaussian plume model for multiple sources are described. They include considerations of diurnal and seasonal variations in the atmospheric stability conditions in the Gifford-Hanna model and spatial variations of wind and stability fields in the Gaussian plume model for multiple sources.

6.1 The refinement of the Gifford-Hanna simple model

In view of the potential of the Gifford-Hanna model to predict mean pollutant concentrations under near-adiabatic conditions it is surprising that the model has not been utilized to its full capacity to include considerations of changing atmospheric stability. Observed diurnal variation of the stability factor C was first used by Hanna (1977) to determine mean concentrations of carbon monoxide in several parts of the United States. By contrast, the application of the Gifford-Hanna simple model to estimates of SO_2 levels has been limited to atmospheric conditions of neutral stability. As the value of the factor C is known to vary with the pollutant species (Gifford and Hanna, 1973), being generally lower for sulphur dioxide than for inert pollutants such as carbon monoxide, there is a need to investigate the diurnal and seasonal cycle in the magnitude of C separately with respect to SO_2 concentrations.

6.1.1 The diurnal variation of the stability factor

Hourly values of wind speed and SO_2 concentrations were measured at seven sites in Pretoria during the winter 1977. Figure 6.1 shows the mean diurnal variation of the concentration in the city

centre (Station No. 18). As has been reported by Halliday and Kemeny (1964) and Kemeny and Halliday (1972) for Pretoria, Tyson (1964) for Johannesburg, DSIR (1945) for Leicester, U.K., Munn and Katz (1959), Summers (1961) and Munn and Ross (1961) for different localities in the United States and Canada and by Zanetti et al.(1977) for Venice, Italy, two peaks are apparent in the hourly variation of sulphur dioxide and smoke concentrations: one a few hours after sunrise, the other just after sunset.

The diurnal variation of wind speed in Pretoria follows the usual pattern reported by Holland and Myers (1953), De Marrais (1961b), Crawford and Hudson (1970) and others for many places in the world, and by Tyson (1968, 1969) and Tyson and Keen (1970) for various localities in South Africa (Figure 6.2). The period of light winds in the early hours of the day is followed by increased wind activity reaching the peak in the early afternoon and falling off gradually to the nocturnal level by about 20h00.

Using the hourly observations of SO_2 concentrations and wind speed, hourly values of the factor C have been determined from the equation

$$C = \frac{u \cdot \chi_A}{q} \qquad (6.1)$$

The relative contribution χ_A by the area sources to the total observed concentration χ has been estimated from the application of the ATDL-grid model at each point of observation. The rate of emission q from the area sources varies in space but is assumed to be invariant in time. The results represent local mean values of C over the period of approximately one month. The overall diurnal variation is obtained by spatially averaging over all seven stations. Figure 6.3 shows the resulting curve of normalized hourly mean variation of the factor C.

The information on the diurnal variation of C in Figure 6.3 can be used in the model to predict pollutant concentrations when equivalent information concerning the emission rate and the mean wind speed is available. In order to investigate the validity of the model predictions, the model has been applied

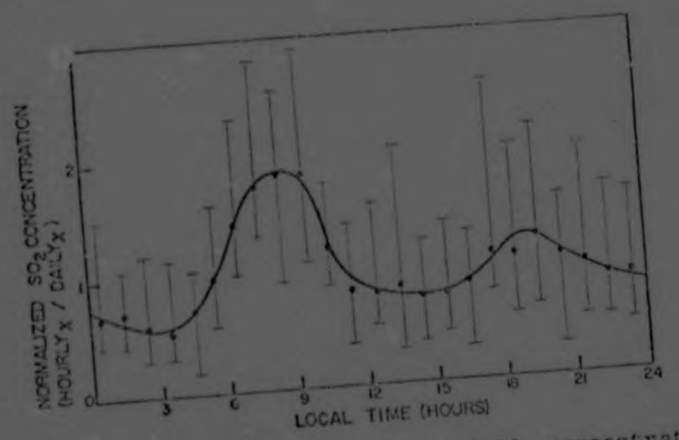


Figure 6.1 Observed diurnal variation of SO_2 concentrations in Iretoria (Station No. 18) during winter 1977

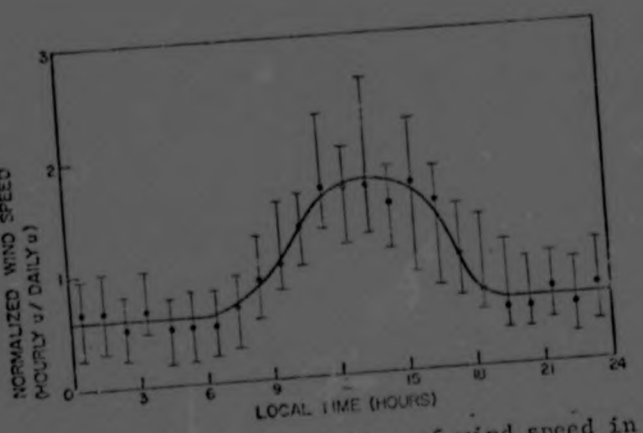


Figure 6.2 Observed diurnal variation of wind speed in Pretoria (Site No. 1) during winter 1977

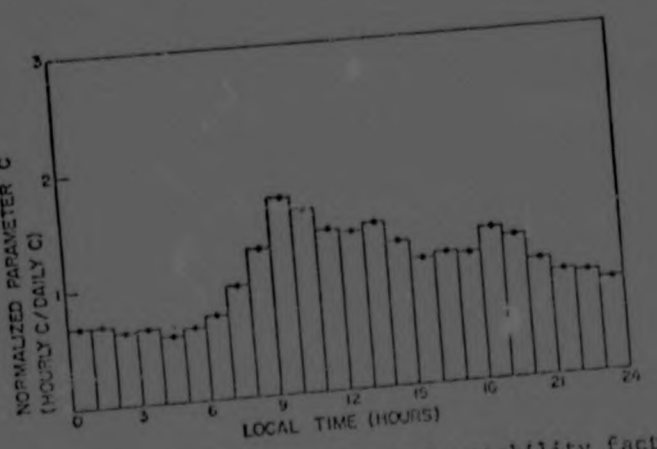


Figure 6.3 Mean diurnal variation of the stability factor in Pretoria during winter 1977

to a data set other than the original one used in the course of the derivation. A detailed search for independent data has revealed that the best available information which could be used for the verification is a series of measurements carried out during the winter season 1969 in Pretoria by Kemeny and Halliday (1972). The measurements include hourly mean values of wind speed and SO_2 concentrations at a site in the central business district. However, the available information does not include an estimate of SO_2 emission rates for 1969. The emission inventory for winter 1977 has been used instead in the process of validation.

The use of a later emission inventory is not expected to influence significantly the spatial and temporal distribution of atmospheric sulphur dioxide as the location of the sources and the diurnal pattern of emissions during the same season are known not to have changed over the eight-year period. The intensity of emissions is likely to have changed owing to changes in consumption, production rates, installation of new equipment and the chemical composition of the combustable fuels. An indication of the magnitude of the difference in the emission intensity may be obtained using observed concentrations reported by Kemeny (1979) in an analysis of long-term trends in sulphur dioxide levels. A comparison of the mean winter SO_2 concentrations in Pretoria shows an increase of between ten to twenty percent from 1969 to 1977. As the actual difference in the emission rates will be of the same magnitude, the use of the 1977 emission inventory in the 1969 data set does not invalidate the results of the following evaluation.

The contribution by area sources to the winter 1969 SO_2 concentration at station No.1 in Pretoria has been calculated from the emission and wind data and the hourly values of C in Figure 6.3. The contribution by point sources has been estimated using the Gaussian plume model and accounted for about 13 percent of the total predicted value. A comparison of the predicted mean diurnal variation of SO_2 concentrations for June 1969 with observations in Figure 6.4 indicates a close association between the two. In addition to simulating the mean diurnal variation over a period of a month, selected case studies have been used to assess the performance of the diurnal

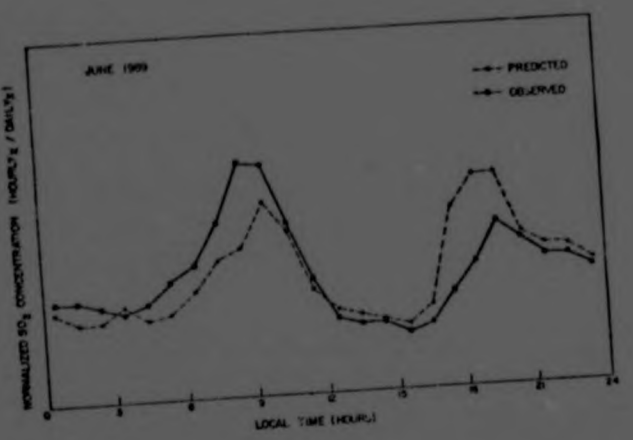


Figure 6.4 Comparison of the estimated and measured diurnal variation of SO_2 concentrations in Pretoria during June 1969

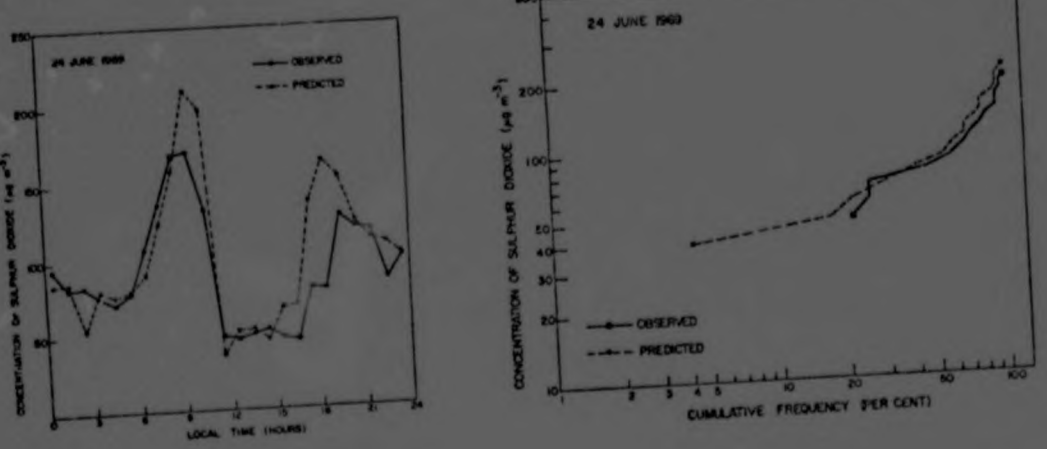


Figure 6.5 Comparison of estimated and measured SO_2 concentrations in Pretoria on 24 June 1969

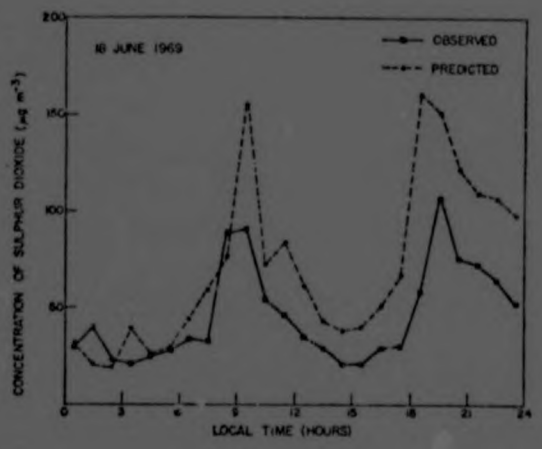
model in more detail.

24 June 1969

The wind conditions observed on 24 June 1969 correspond closely to the mean winter pattern given in Figure 6.2. Outside the period of convective activity during the hours of intensive solar radiation, the wind speed was low and the wind direction uniform and steady. Comparison between the predicted and observed hourly concentrations of sulphur dioxide for the 24-hour period is shown in Figure 6.5. The correlation coefficient between the two sets of data is 0,83 and the mean relative deviation of the predicted values from the observations is 12,3 percent, indicating a close approximation to the observed temporal pattern by the model predictions. The slight overall overestimation by the model may be attributed to the higher emission rates which have been derived from the 1977 information.

18 June 1969

On this occasion the observed temporal pattern of diurnal variations was well approximated by the model predictions (Figure 6.6) yielding a correlation coefficient of 0,85. In contrast to the previous application, the overall overestimation by the model is more pronounced and cannot be explained on the basis of 10 to 20 percent innacuracies in the emission estimates alone. In this case, the mean relative deviation of the predicted values from the observations is 55,4 percent. The relationship between the variables in the model equation indicates a linear response of the predicted concentration to changes in the ratio (q/u) and in the factor C. Hence, the overprediction by the model shown in Figure 6.6 can also be induced by an underestimation of the magnitude of wind speed at the site of application or by an overestimation of the value of C. The systematic nature of the prediction error suggests that a slight general overestimation of C in combination with the use of higher emission rates are responsible for the increase of the deviation.



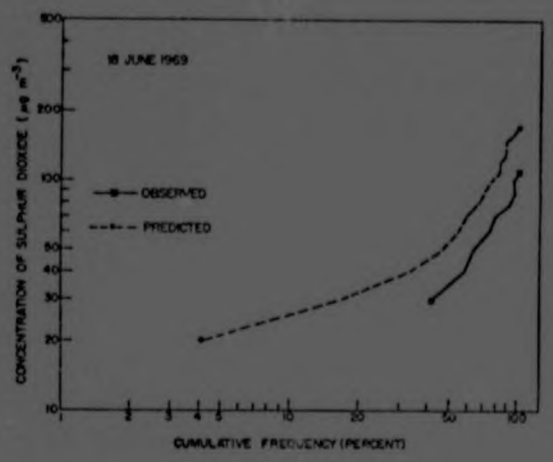


Figure 6.6 Comparison of estimated and measured SO_2 concentrations in Pretoria on 18 June 1969

4 - 5 August 1969

The comparison between the predicted and observed hourly concentrations for the period of 4 - 5 August 1969 in Figure 6.7 shows a high degree of correspondence except in the late evening of 4 August 1969. The observed concentration rose sharply from about 20h00 to 23h00 and reached a peak value of 150 $\mu g/m^3$ shortly before midnight. Thereafter the observed concentration began to decrease and close agreement between the observations and the predictions was re-established at about 02h00 on 5 August 1969. The magnitude and time of the evening peak of 4 August must be regarded as an isolated and anomalous phenomenon caused by a distinct change in dispersion conditions not reflected in the model. The mean hourly values of wind speed and wind direction during the period of interest were recorded at a nearby site and are shown in Figure 6.8. During the morning of 4 August, generally low wind conditions prevailed until approximately 09h00 when the established mean pattern in the wind speed cycle began to develop. The wind speed, however, failed to return to its nocturnal level and a sharp increase was observed at 17h30. The sudden increase of speed was associated with a change of the wind direction by more than 100 degrees (Figure 6.8). By about 02h00 on 5 August 1969, both the wind speed and direction returned to the levels observed during the previous night. Hence, the observed peak in the sulphur dioxide concentration during the period of local disturbance of wind flow can best be explained by transport of the pollutants from a strong source which was situated directly upwind the receptor when the wind direction changed.

6.1.2 The seasonal variation of the stability factor

In order to determine seasonal variations of the stability factor C in the Gifford-Hanna simple model experimentally, it would be necessary to maintain the monitoring network fully operational throughout the year and record mean values of SO_2 concentrations and wind speed simultaneously at a number of stations. The maintenance of such a monitoring network not being feasible, an al-

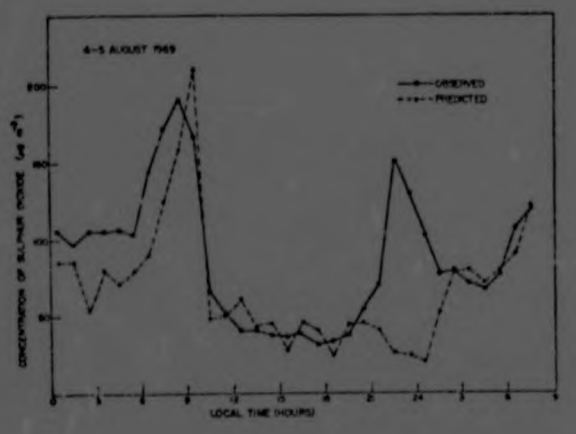


Figure 6.7 Comparison of estimated and measured SO_2 concentrations in Pretoria on 4-5 August 1969

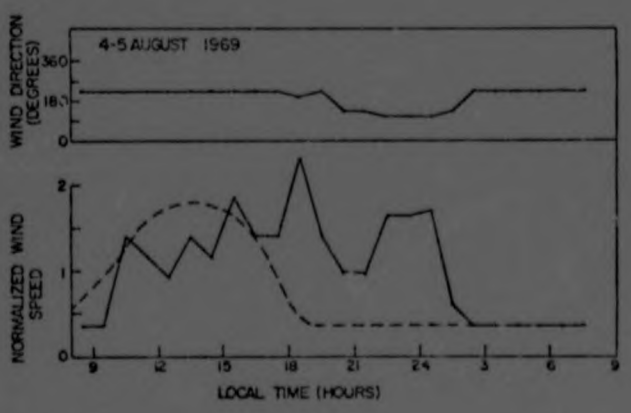


Figure 6.8 Observed variation of wind direction and speed in Pretoria on 4-5 August 1969. The dotted line shows the mean wind speed cycle in winter

ternative approach has been adopted, in which an objective weighting scheme is employed to determine the seasonal variations of C, using only a limited amount of data. The hourly winter values of C have been integrated into daily and monthly averages for each pair of observations (Table 6.1). The mean winter value for the whole of Pretoria has been calculated as the arithmetic mean $\bar{C}$ = 55,3 with a standard deviation of 17,3.

Table 6.1. Experimentally determined winter 1977 values of the stability factor C in Pretoria

Monitoring station (number)		Area source strength	Rel. contribution of area sources	$C = \frac{u\chi_A}{q}$
SO_2	Wind	($\mu g/m^2$ s)	(χ_A/χ)	
No.18	No.1	1,43	0,88	76,0
13	12	0,02	0,01	30,0
16	11	0,07	0,08	69,9
17	4	2,34	0,97	39,2
12	1	1,25	0,85	38,8
14	2	0,95	0,55	62,9
10	13	0,46	0,51	70,5
Mean				55,3
Standard deviation				17,3

The seasonal variation of C is estimated by weighting the observed winter value against the information on the variation of occurence of individual stability categories during each season.

It has been shown earlier that for an area of constant size the factor C is a function of the atmospheric stability, viz.

$$C = \left(\frac{2}{\pi}\right)^{\frac{1}{2}} \frac{D^{1-b}}{a\,(1-b)}$$

Variations of C with stability categories can therefore be expressed as a ratio

$$\gamma(i) = \frac{C\ (i)}{C\ (R)} \qquad (6.2)$$

where C(i) represents the value of C for an arbitrary stability category i and C(R) is the value of C for a reference stability category R. The seasonal variations of the factor C are then determined by the frequency of occurence of each stability category during the period of interest. If f(i,j) denotes the frequency of occurence of the i-th stability category in the j-th season and C(W) represents the observed value of C during the reference season W, then the mean value of C in the j-th season is weighted against the observed value C(W) as

$$C\ (j) = C\ (W)\ \frac{\sum_i \gamma(i)\ f(i,j)}{\sum_i \gamma(i)\ f(i,W)} \qquad (6.3)$$

This objective weighting scheme has been used to extend the applicability of the Gifford-Hanna simple model to predictions of concentrations over periods of differing stability conditions. Stable conditions represent the reference state of the atmosphere during the winter season. The frequency of occurence of six Pasquill stability categories has been estimated from observations at the wind recording site No. 2 for every season of 1977. The Pasquill stability categories have been reduced to three classes representing the unstable (Pasquill A, B, C), neutral (D) and stable (E, F) atmospheric conditions. The ratio γ (i) has been determined for these stability classes and a mean upwind city size of 10 kilometres. Table 6.2 shows the seasonal values of C calculated from the weighting scheme in Equation (6.3) and using the observed winter value of C (W) = 55,3.

In order to verify the seasonal model the simulation of known 1969 SO_2 concentrations at station No.1 in Pretoria has been undertaken. Mean seasonal values of wind speed and the strength of area sources in the central business district have been used along with the seasonal values of C in Table 6.2 to calculate the contribution by low-level sources to the total concentration in central Pretoria.

Table 6.2 Estimated seasonal variation of the stability factor C in Pretoria

Period of time	Calculated value of C	Rounded value of C
Winter	55,3	55
Spring, summer, autumn	19,7	20
Semi-annual (June-November)	37,5	35
Annual	28,8	30

The contribution by elevated point sources has been added by invoking the standard Gaussian plume formula. The total predicted 1969 concentrations for time intervals ranging from a month to a year are all within 20 percent of observed concentrations (Table 6.3).

The application of the seasonal Gifford-Hanna model has further been extended to the 1977 data to examine its performance in relation to the performance of other models of comparable degree of simplicity. Table 6.4 shows a comparison of the performances of the ATDL-grid model and the seasonal Gifford-Hanna model for differing time intervals during 1977. The improvement of correlation results for the seasonal Gifford-Hanna model is both significant and consistent. The correlation coefficient increases by as much as 0,33 from 0,52 for the ATDL-grid model to 0,85 for the seasonal Gifford-Hanna model during the six-monthly interval. A reduction by 68 percent in the standard error from 81,6 $\mu g/m^3$ to 26,1 $\mu g/m^3$ is achieved by the seasonal Gifford-Hanna model in winter 1977.

6.1.3 Discussion

The applicability of the Gifford-Hanna simple model has been extended from the simulation of long-term atmospheric pollution

Table 6.3 Comparison of observed and predicted mean SO_2 concentrations by the seasonal Gifford-Hanna model during 1969 at station No.1 in Pretoria

Period of time	Area sources				Point sources	Total SO_2 concentration	
	Mean wind speed (m/s)	Emission rate ($\mu g/m^2$ s)	Factor C	Mean concentration ($\mu g/m^3$)	Mean concentration ($\mu g/m^3$)	Predicted ($\mu g/m^3$)	Observed ($\mu g/m^3$)
Annual 1969	1,50	0,82	30	16,4	4,7	21,1	25
Winter 1969	1,24	1,43	55	63,3	8,9	72,2	60
June 1969	1,28	1,43	55	61,4	10,3	71,7	65

Table 6.4 Comparison of the performance of the ATDL-grid model and the seasonal Gifford-Hanna model during 1977 in Pretoria

Time interval	3 Months (Winter 1977)			3 Months (Spring 1977)			6 Months (June-November 1977)		
Type of model	Standard error ($\mu g/m^3$)	Mean deviation	Correlation coefficient	Standard error ($\mu g/m^3$)	Mean deviation	Correlation coefficient	Standard error ($\mu g/m^3$)	Mean deviation	Correlation coefficient
Grid model	81,6	+1,50	0,55	8,7	-0,02	0,72	18,4	+0,39	0,52
Simple seasonal model	26,1	+0,46	0,70	7,8	-0,23	0,84	8,1	+0,03	0,85

levels under near-neutral stability conditions to predictions of seasonal variations in the concentrations of the order of one month and longer. A seasonal variation of the factor C which is used in the Gifford-Hanna simple model to estimate the concentration in proportion to the ratio of the grid emission rate to the mean wind speed in the area, has been introduced. The winter value of C has been determined from observations of SO_2 concentrations and wind speed at several urban sites. Using this value as a reference value, an objective weighting scheme has been applied to derive the seasonal variation of C from observations of atmospheric stability in each season. The verification of the seasonal model has clearly stressed the potential of the Gifford-Hanna simple model as a predictive technique. A consistent improvement over the ATDL-grid model has been obtained. Although a direct application of the specific values of C as determined for Pretoria may not always be possible for other cities, the simple seasonal model is applicable in principle to any urban area. A simple experiment may be designed to validate or to adapt the magnitude of C during the reference season in the specific area.

The manner in which the Gifford-Hanna simple model may be employed on an hour-by-hour basis has also been shown. A mean diurnal variation of the stability factor C is used together with hourly estimates of mean wind speed and grid emission rate to determine the contribution by low-level area sources. Large point sources are treated separately by the Gaussian plume model. The simple diurnal model has been verified using an independent set of 1969 data. The results indicate a close correspondence of model predictions to the observed temporal pattern for most of the time. Whereas the model can handle wind variations which approximate the mean diurnal cycle of velocity, it cannot cope with sudden changes induced by synoptic disturbances. Although the mean diurnal cycle of wind speed and SO_2 concentrations in many other cities is reported to follow a similar pattern to that used in the derivation of C in Pretoria, a direct application of the numerical values of C for other urban areas must be approached with caution. Initially, a simple experiment may be necessary to validate the mean pattern of variation and the magnitude of C.

6.2 The refinement of the Gaussian plume model for multiple sources

All attempts to include spatial variations of wind vector and atmospheric stability in the Gaussian plume model are encumbered by the complexity of the so-called windfield models which are used to describe the transport and dispersive capacity of the planetary boundary layer. In the absence of windfield models simple enough to be incorporated into a Gaussian dispersion model, the increased number of wind and stability observations in the area may be used as a surrogate measure to approximate the real changes of the meteorological parameters in the shallow layer above the ground. Using multiple observations, spatially and temporally variable fields may be constructed by applying interpolative schemes. In the interpolative schemes the value of a meteorological variable P at a point of interest (x, y) is estimated as a weighted average of the measured data at S observation sites. If W_s (t) denotes the weighting factor of the observation at the site s and time t, the interpolated horizontal component of F may be expressed as

$$P(x,y,t) = \frac{\sum_{s=1}^{S} P_s(t)\ W_s(t)}{\sum_{s=1}^{S} W_s(t)} \qquad (6.4)$$

where $P_s(t)$ is the observed value at the site s and time t.

Wendell (1970) has used a simple time interpolation scheme to determine the wind at the time of interest τ from the preceding observation at time t_1. The weighting factor $W_s(t_1)$ is given as

$$W_s(t_1) = \frac{1}{\tau - t_1} \qquad (6.5)$$

Similarly, the weighting factor for the succeeding observation at time t_2 is

$$W_s(t_2) = \frac{1}{t_2 - \tau} \qquad (6.6)$$

Mc Mullen (1964) has suggested a scheme in which the simple linear relationship is replaced by integrated values of the inverse square

of the time lapse as

$$W_s\ (t_1) = \int_{\tau_1}^{\tau_2} \frac{1}{(\tau - t_1)^2}\ d\tau \qquad (6.7)$$

and

$$W_s\ (t_2) = \int_{\tau_1}^{\tau_2} \frac{1}{(t_2 - \tau)^2}\ d\tau \qquad (6.8)$$

In most applications the required temporal resolution of the wind data may directly be obtained from the record itself. The simplest factor in a space interpolation scheme is one which weights the observed data according to the distance r_s between the station and the point of interpolation, viz.

$$W_s = r_s^{-p} \qquad (6.9)$$

The application of the above scheme with p = 2 has been reported by Wendell (1972), Scholtz and Brouckaert (1976) and others. Smith (1978) has generalized a scheme introduced by Garstang (1977) in which the weighting factor decreases exponentially with the distance as

$$W_s = B_s \exp\left(- k_s \frac{r_s}{r_o}\right) \qquad (6.10)$$

where k_s is an arbitrary constant which determines the cut-off rate in the effect of distant observations and r_o indicates the distance between the point of interpolation and the nearest observation. The parameter B_s allows to assign a lower or a higher weight to observations at a station in relation to the rest of the data set.

6.2.1 The generation of horizontal wind and stability fields

The composite frequency function is used in the Gaussian plume model to characterize the dispersion conditions at a given point in the urban area. If the frequency functions f_s (i, j,) are specified from observations at S meteorological sites, the resulting frequency function at the point of interpolation (x,y)

may be obtained as

$$f_{x,y}(i,j,k) = \frac{\sum_{s=1}^{S} f_s(i,j,k)\ r_s^{-2}}{\sum_{s=1}^{S} r_s^{-2}} \qquad (6.11)$$

The relative significance of each observation to the interpolated frequency function is controlled by the square of the distance r_s between the point of interpolation and the observation site. The application of the interpolation scheme to generate horizontal wind and stability fields in Pretoria is illustrated in Figure 6.9. There are thirteen observation sites at each of which hourly values of wind speed, wind direction and atmospheric stability category are available. When the pollutant concentration is to be estimated at the receptor R, the dispersion conditions at that point are described in the model by the composite frequency function which is determined from Equation (6.11). So for instance, the relative weight of the observation at the site No.4 to the frequency function at the receptor is proportional to the distance as ($1/r_4^{\ 2}$). The nearest observation (Site No. 13) is the most heavily weighted, the most distant observation (Site No.10) is the lightest. By contrast, in the weighted average at the point R' the observation from the site No.10 is the most significant and the observation from the site No.13 is the least significant. By using a network of regularly spaced receptors a horizontal wind and stability field is generated.

The generated horizontal fields have been utilized in the Gaussian plume model to predict the 1977 SO_2 concentrations in Pretoria. At each point of calculation the composite frequency function has first been evaluated on an hourly basis using all thirteen observation stations. Then, the weighted value of the frequency of occurence of sixteen wind sectors, five wind speed classes and six stability categories has been used in the final equation, viz.

$$\chi = \left(\frac{2}{\pi}\right)^{\frac{1}{2}} \left(\frac{n}{2\pi}\right) \sum_{m=1}^{M} \sum_{j=1}^{J} \sum_{k=1}^{K} \frac{Q_m \cdot f(i_m,j,k)}{r_m \cdot u(j) \cdot \sigma_z(r_m,k)} \exp\left[-\frac{H_m^{\ 2}}{2\sigma_z^2(r_m,k)}\right] \exp(-\lambda \Delta t) \qquad (6.12)$$

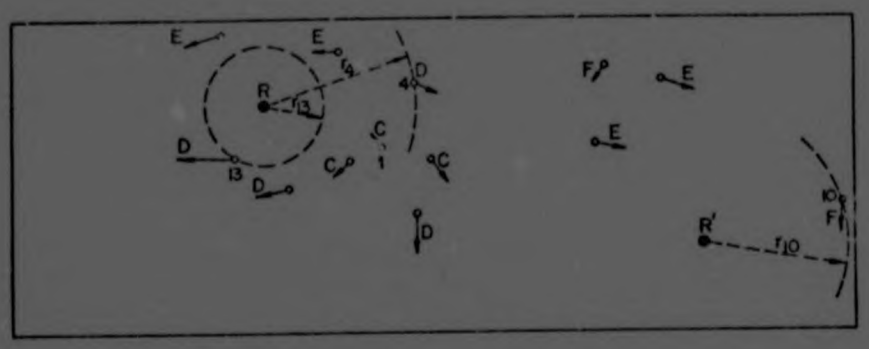


Figure 6.9 Application of an interpolation scheme to generate horizontal wind and stability fields in Pretoria. The arrows show the wind direction and the symbols A-F Pasquill stability categories at observation sites. The points of interpolation are indicated by R, R'

to determine the contribution by all point sources. The same procedure is repeated for the area sources using Equation (4.12). When the total concentration at the receptor has been estimated, the next receptor point is introduced, the corresponding composite frequency function is evaluated and used in the model equations etc. Figures 6.10 and 6.11 show the resulting isopleths of predicted SO_2 concentration for winter and spring 1977. The correlation between individual pairs of predicted and observed values at the stations in Pretoria is shown in Table 6.5 for various time intervals.



Figure 6.10 Isopleths of SO_2 concentration ($\mu g/m^3$) estimated for winter 1977 in Pretoria by the refined Gaussian plume model for multiple sources. Cross symbols indicate the stations at which wind data have been recorded for the simulation

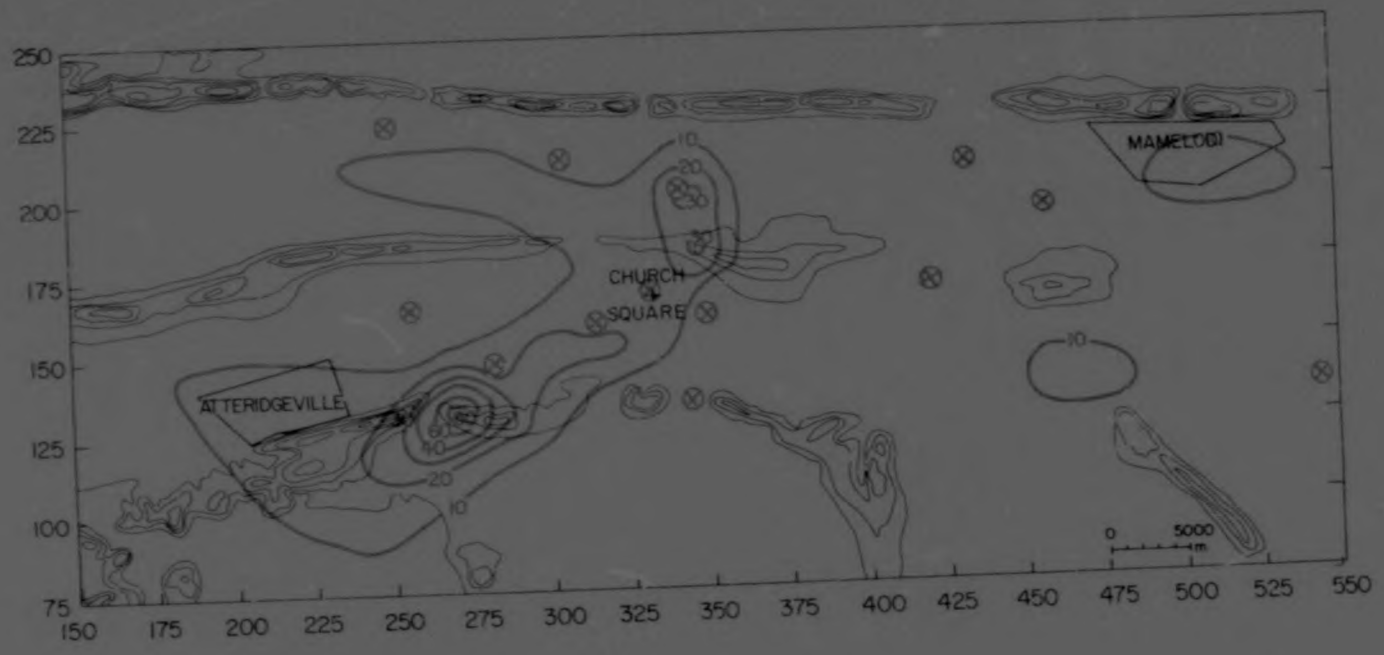


Figure 6.11 Isopleths of SO_2 concentration ($\mu g/m^3$) estimated for spring 1977 in Pretoria by the refined Gaussian plume model for multiple sources

Table 6.5 Comparison of observed and predicted SO_2 concentrations ($\mu g/m^3$) by the refined Gaussian plume model for multiple sources in Pretoria

Station number and grid position	1 Month (July 1977)			1 Month (November 1977)			3 Months (Winter 1977)			3 Months (Spring 1977)			6 Months (June-Nov 1977)		
	Obs.	Pred.	Rel. dev.	Obs.	Pred.	Rel. dev.	Obs.	Pred.	Rel. dev.	Obs.	Pred.	Rel. dev.	Obs.	Pred.	Rel. dev.
1 (335;163)	62	55	-0,11	24	10	-0,58	59	53	-0,10	28	16	-0,32	43	28	-0,35
2 (341;157)	52	27	-0,48	14	7	-0,50	47	28	-0,40	18	10	-0,45	31	18	-0,42
3 (335;188)	38	43	+0,13	12	14	+0,17	34	42	+0,24	19	22	+0,16	26	32	+0,23
4 (354;162)	39	17	-0,56	22	6	-0,73	36	18	-0,50	20	9	-0,55	28	13	-0,53
5 (426;167)	22	10	-0,55	9	2	-0,78	18	11	-0,39	11	4	-0,64	14	7	-0,50
6 (286;129)	31	31	0,00	32	33	+0,03	36	34	-0,06	30	27	-0,10	33	31	-0,06
7 (265;133)	74	73	-0,01	38	56	+0,47	65	63	-0,03	31	57	+0,84	48	62	+0,29
8 (311;130)	38	22	-0,42	25	7	-0,72	36	21	-0,42	25	9	-0,64	28	15	-0,46
9 (254;117)	34	22	-0,35	28	26	-0,07	29	20	-0,31	27	31	+0,15	35	24	-0,31
Correlation coefficient	0,87			0,81			0,87			0,70			0,79		
Mean rel. deviation	-0,26			-0,30			-0,22			-0,18			-0,24		
Standard error	10,8 $\mu g/m^3$			10,9 $\mu g/m^3$			9,2 $\mu g/m^3$			12,5 $\mu g/m^3$			10,5 $\mu g/m^3$		

6.2.2 Discussion

The spatial variations in the transport and dispersive properties of the atmosphere have been approximated by a simple interpolation scheme in which horizontal wind and stability fields are generated from multiple meteorological observations. The measure of realism in the generated wind and stability fields is influenced by the density of the observations. Table 6.6 shows a consistent improvement in the correlation between predicted and observed SO_2 observations in Pretoria when an increasing number of meteorological observations are used.

The aim of the interpolative scheme has been to provide a relatively simple information for use in the Gaussian plume model without considerably increasing the model complexity and computer running times. By making use of the composite frequency function which combines the wind vector with the degree of static stability, a balance between the transport and dispersion terms is maintained at each point in the urban area. This balance, however, only applies to the horizontal component of the transport term as no considerations are given in the model to changes of wind direction with height. By contrast, the variation of wind speed with height is included in the model by invoking the power law for wind profile.

In order to review the performances of individual urban air pollution dispersion models in the Pretoria situation, and to illustrate the improvements in the accuracy of predictions which have been achieved by the refinements described in this chapter, a summary of the correlation between predicted 1977 concentrations by each examined model and corresponding observations is shown in Table 6.7.

When multiple meteorological observations are used to generate wind and stability fields in the Gaussian plume model, a reduction of the standard error of estimate and an increase of the correlation coefficient are consistently obtained as compared to the performance of the original Gaussian plume model. A higher degree of improvement in the model performance has been achieved for the spring season than for the other time intervals

Table 6.6 Correlation between predicted and observed SO_2 concentrations in Pretoria when an increasing number of meteorological observations are used to determine the composite frequency function in the Gaussian plume model for multiple sources

Time interval	3 Months (Winter 1977)			3 Months (Spring 1977)			6 Months (June-November 1977)		
Number of meteorological observations	Standard error ($\mu g/m^3$)	Mean deviation	Correlation coefficient	Standard error ($\mu g/m^3$)	Mean deviation	Correlation coefficient	Standard error ($\mu g/m^3$)	Mean deviation	Correlation coefficient
1 site	10,6	-0,09	0,86	20,8	+0,07	0,63	14,5	-0,08	0,77
3 sites	12,8	-0,15	0,86	15,4	-0,10	0,66	11,0	-0,18	0,78
13 sites	9,2	-0,22	0,87	12,5	-0,18	0,70	10,5	-0,24	0,79

during 1977.

The performance of the refined Gifford-Hanna simple model may be measured by its comparison to the performance of the original Gifford-Hanna model as well as to that of the ATDL-grid model. Both versions of the Gifford-Hanna simple model give significantly better results than the ATDL-grid model. The highest degree of improvement has been achieved for the winter season. Although the improvement of the prediction results for the only time interval for which the original and refined versions of the Gifford-Hanna simple model can be compared is not significant, the major improvement of the refined model rests in the extension of the predictions to estimates of seasonal and diurnal concentration levels.

Finally, the summary of the performances in Table 6.7 shows that the refined Gifford-Hanna simple model predicts concentration levels of sulphur dioxide in the Pretoria urban area with a degree of success that is comparable to the performance of the Gaussian plume model for multiple sources. In fact, the performance of the Gifford-Hanna simple model in Pretoria has been slightly better for two out of the three time intervals examined.

Table 6.7 Comparison of the performances of the original and refined urban air pollution dispersion models in Pretoria

TIME INTERVAL		3 MONTHS (Winter 1977)			3 MONTHS (Spring 1977)			6 MONTHS (June - November 1977)		
MODEL		Standard error ($\mu g/m^3$)	Mean deviation	Correlation coefficient	Standard error ($\mu g/m^3$)	Mean deviation	Correlation coefficient	Standard error ($\mu g/m^3$)	Mean deviation	Correlation coefficient
Gaussian plume model	Original	10,6	-0,09	0,86	20,8	+0,07	0,63	14,5	-0,08	0,77
	Refined	9,2	-0,22	0,87	12,5	-0,10	0,70	10,5	-0,24	0,79
ATDL-grid model		81,6	+1,50	0,55	8,7	-0,02	0,72	18,4	+0,39	0,52
Gifford-Hanna simple model	Original	Not applicable			Not applicable			8,8	+0,23	0,85
	Refined	26,1	+0,46	0,70	7,8	-0,23	0,84	8,1	+0,03	0,85

PART IV - CONCLUSIONS

CHAPTER 7

SUMMARY

An exact mathematical description of pollutant dispersion in city atmospheres is made impossible by the intractability of the basic equations derived for the atmosphere from the principles of conservation of mass, momentum and energy. Several approaches have been proposed in which various degrees of idealizations are introduced with the aim of obtaining approximate solutions for use in dispersion models. The theoretical difficulties are often compounded by the multitude of input information which is required for the execution of a computerized model and by the computational effort involved in the simulation. As a result a variety of urban dispersion models have been developed for a wide range of applications concerning the atmospheric pollution of cities.

In this thesis the use of mathematical modelling of urban air pollution has been reviewed. Attempts have been made to identify critical parts of dispersion models in general, to evaluate the performance of Gaussian models of a varying degree of simplicity in Pretoria and to delimit and to refine dispersion models for practical use in South African conditions. The specific results of the investigation can be itemized as follows:

A. APPROACH TO MODELLING URBAN AIR POLLUTION

1. Based upon a careful review of existing urban air pollution models it has been shown that a whole spectrum of models must be considered for application to the city atmospheric environment. This is contrary to modelling dispersion of atmospheric pollutants from isolated sources for which the Gaussian model is widely accepted as the best applicable approach.

2. In regression models statistical analysis of a number of variables is used for estimates of future concentration levels at a specific locality in the city. The regression models give

a quick answer in applications where the possible effect of a change in a major variable such as the emission rate is the main consideration.

3. A simplistic approach to the physical basis of pollutant dispersion has been taken in the box model and the ATDL-grid model. The simple models are best suitable for predicting mean concentrations in urban areas in which the emissions are evenly distributed and the variations in emission rates with position are small.

4. The Gaussian models, with their assumption of normal distribution of pollutants in the atmosphere, have become the most widely applied technique for describing dispersion of quasi-stable pollutants in steady-state conditions. In contrast to the plume model, the puff model can handle dispersion under low wind conditions which often lead to a build-up of pollution in cities.

5. The principle of mass conservation is the basis of the gradient transport models in which the dispersion is related to the gradient of pollutant concentration. The main domain of these models is the simulation of the behaviour of chemically active pollutants in the city air.

6. The main characteristics of urban air pollution dispersion models and fields of their application are summarized in Table 7.1. Three of these, the Gaussian plume model for multiple sources, the ATDL-grid model and the Gifford-Hanna simple model have been investigated in greater detail in the Pretoria urban area.

Table 7.1 Summary of the main characteristics of urban air pollution dispersion models and the fields of their application

	REGRESSION MODELS		SIMPLE MODELS		GAUSSIAN MODELS		GRADIENT TRANSFORT MODELS	
	Proportional	Empirical	Box	ATDL	Plume	Puff	Analytical	Numerical
Degree of detail required from the input data	small	small	small	small	large	large	large	large
Computer time required for the execution	none	none	none	none to little	little to extensive	extensive	little	extensive
Spatial resolution of results	none	none	none to poor	poor	good	good	good	good
Temporal resolution of results	poor	poor	poor	poor to good	good	good	good	good
General applicability of the model	none	none	poor	poor	poor to good	poor to good	poor	poor to good
Main fields of application	local problems testing complex models		integral problems testing complex models		detailed predictions research		detailed predictions chemically active pollutants research	

B. THE GAUSSIAN PLUME MODEL FOR MULTIPLE SOURCES

1. The Gaussian plume model realistically simulates long-term concentrations of atmospheric sulphur dioxide in the Pretoria urban area. Likewise it has been shown that the performance of the model does not significantly vary with seasonally induced changes in dispersion conditions.

2. The occasional occurence of higher deviations in predicted values of air pollution at some of the receptors in the area has indicated that the sound overall performance of the model cannot be interpreted as a proof of its capacity to estimate pollution levels at all sites with the same degree of accuracy. The accuracy of predictions at individual sites is affected by the treatment of the spatially variable wind and stability fields in the model.

3. When single-point meteorological measurements are used to represent the dispersion field within the whole city in the original Gaussian plume model for multiple sources, the subjective selection of the observation site has been shown to become an important factor in the model. In the case of Pretoria, the mean relative deviation of predicted from observed SO_2 concentrations varies with the location of the single-point measurement from -73,2 percent to +48,3 percent of the observed values.

4. A consistent improvement in the correlation between predicted and observed air pollution levels is obtained when an increasing number of wind and stability observation sites are used to simulate spatial variations in the dispersion conditions over Pretoria. The multiple meteorological observations have been used in an interpolation scheme to generate horizontal wind and stability fields in the urban area.

5. It has been shown that the interpolation scheme can successfully be employed in the Gaussian plume model without significantly increasing the model complexity and computer running times.

6. A balance between the transport and dispersive properties of the atmosphere has been maintained in the model by using a composite function which combines the wind vector with the degree of static stability at each point in the urban area.

7. In contrast to the situation in the real atmosphere, the supposition that the wind does not change direction with height has been retained in the model. As it has been shown that the distribution of pollutant concentration in a city is dominated by the low-level sources, this deficiency is not expected to invalidate the results of future applications of the model.

C. THE ATDL-GRID MODEL

1. It has been shown that the model does not adequately simulate air pollution levels during the winter, the main pollution season in the Pretoria urban area. A significant overestimation by the factor of three to four has consistently been found at receptors in or near the central business district where a large number of low-level souces are situated.

2. The treatment of the low-level emission sources as ground-level emissions in the model is the main reason for its unsatisfactory performance. During the winter most of the low-leval sources are active when unfavourable dispersion conditions prevail associated with the development of strong surface-based inversions and low wind speeds. It is under these conditions that the real physical height of the low-level sources becomes the decisive factor in the ultimate distribution of the emitted pollutant.

3. Attempts to include considerations of the real emission height lead to a complex equation for area sources which is in direct contradiction to the required relative simplicity of the ATDL-grid model. The concept of defining a spatially invariable mean wind vector for the whole city and the absence of the removal term from the model equation contribute to the reduced performance of the model.

4. Being of unsatisfactory performance and of little potential for improvement, the ATDL-grid model has been rejected for the Pretoria situation.

D. THE GIFFORD-HANNA SIMPLE MODEL

1. The suggestion that the analytical description of area sources in the ATDL-grid model can successfully be replaced by estimating the pollutant concentration in proportion to the ratio of the integrated emission rate in the grid square to the mean wind has been confirmed.

2. By determining the factor of proportionality empirically, the antagonism between the real emission height of urban sources and the concept of ground-level sources in the ATDL-grid model is eliminated. The applicability of a constant value of the factor C to represent the mean semi-annual and annual dispersion conditions over an urban area has been confirmed.

3. Exploiting the implicit dependence of the concentration distribution on variations in atmospheric stability, the Gifford-Hanna simple model has been refined to include time scales over which the mean dispersion conditions cannot be approximated by the neutral state as reflected in the use of a constant value of C. The time scales cover

the mean hourly and the mean monthly to seasonal distribution of pollutant concentration.

4. The major improvement in the applicability of the refined model rests in its extension to estimates of hourly to annual concentrations while retaining the simplicity of the original model.

5. A seasonal variation with discrete stability categories has been introduced into the model using an objective weighting scheme. In the seasonal model the observed winter value of the stability factor C is weighted against the variation of occurence of individual stability categories in each season.

6. The seasonal model has shown a significant and consistent improvement in the quality of concentration predictions against the ATDL-grid model.

7. Likewise it has been shown that a mean diurnal variation of C can be used in the Gifford-Hanna simple model together with hourly estimates of grid emission rates and mean wind speed to simulate the variation in the pollutant concentration on an hour-by-hour basis.

8. The model has been verified and shown to be capable of handling wind variations which approximate the mean diurnal cycle of velocities. By contrast to the successful simulation of the mean diurnal cycle, the model is unable to cope with sudden changes induced by synoptic disturbances to the mean flow pattern.

9. It has been shown that the refined Gifford-Hanna simple model predicts concentration levels of atmospheric sulphur dioxide in the Pretoria urban area with a degree of success that is comparable to the performance of the Gaussian plume model for multiple sources.

E. METHODOLOGY OF FUTURE MODELLING APPLICATIONS

1. A selective choice of the appropriate dispersion model is essential in future modelling applications designed to predict concentration levels of atmospheric pollutants in South African cities. The standard Gaussian plume model for isolated sources provides a reliable basis for simulating the production of ground-level concentrations from large elevated point sources.

2. A wider selection of applicable models exists for estimating pollution levels resulting from the emissions from low-level urban sources. The Gaussian

plume model for multiple sources may successfully be employed to predict long-term concentrations of quasi-stable pollutants. The use of multiple meteorological observations in the model will improve the realism of individual predictions in urban areas where dispersion conditions vary markedly with position in the city.

3. The requirements on input data collection and computer running times for the Gaussian plume model increase considerably when a high spatial resolution of predicted pollutant concentrations is desired. High total cost of the simulation must therefore be expected.

4. The refined Gifford-Hanna model, on the other hand, provides a fast and inexpensive methodological basis for predicting hourly, monthly, seasonal and annual air pollution levels from multiple urban sources, especially in applications where modest requirements on the data acquisition programmes and low costs are the main considerations.

5. In addition to the selection of the appropriate type of model, the accuracy of dispersion estimates is dependent upon the accuracy and representativeness of the input parameters. A careful monitoring and a correct use of input data have been shown to constitute an important step in the methodology of dispersion modelling.

6. The experimental programmes designed to collect data for model implementation may be rationalized by analyzing the sensitivity of the model to variations in the input parameters. A cost-effective application of a mathematical dispersion model can be achieved without reducing the accuracy of predicted concentrations of air pollution by emphasizing the monitoring of those parameters to which the model is most sensitive and by limiting the monitoring of the remaining input.

7. The sensitivity analysis of the Gaussian plume model for multiple sources has shown that the predictions of concentration levels of sulphur dioxide are most sensitive to variations in the emission rates, the vertical dispersion coefficient σ_z and the variables in the composite frequency function, i.e. the wind speed, wind direction and atmospheric stability.

8. Random errors of the order of magnitude in the input data have been shown to have little effect on the prediction results in the multiple-source environment of a city. By contrast, systematic errors in the input, even of a lesser magnitude than the random errors, have been shown to have a significant effect on the dispersion estimates.

In this thesis mathematical modelling of air pollution dispersion in urban areas has been investigated. No substantial evidence has been found to suggest the existence of a uniquely applicable dispersion model. In general, the selection of the best applicable model is dictated by the nature of the specific problem, the availability of suitable experimental data and computing facilities. Such has been the case in the Pretoria study. On the basis of the research carried out, the often expressed notion that simple models cannot provide a satisfactory description of atmospheric pollution in urban areas must be rejected. On the contrary, the performance of the refined Gifford-Hann simple model in the Pretoria urban area has been slightly better than the performance of the Gaussian plume model for multiple sources for two out of three time intervals examined. The simple models are, however, subject to large errors if applied indiscriminately to dispersion estimates under anomalous atmospheric conditions.

A substantial improvement on the immediate past usage of the Gifford-Hanna simple model has been made by developing seasonal, monthly and hourly equivalents of the original annual model. The ways in which this has been achieved had on purpose been chosen to be simple and inexpensive. The Gaussian plume model for multiple sources has likewise been refined by including horizontal wind and stability fields in the dispersion model. Once again, a simple interpolation scheme is used to derive the information from inexpensive meteorological observations. In addition to these contributions several aspects concerning air pollution modelling in a new area of application have been elucidated.

One of the main objectives of the thesis was to provide a basis for future urban air pollution modelling in South Africa. This has been done and two models of varying degrees of simplicity, the Gaussian plume model for multiple sources and the Gifford-Hanna simple model, have been evaluated, refined and verified using Pretoria as a model city. Owing to its valley situation the Pretoria area is effectively sheltered from outside interference by large-scale air movements and steady, well-defined atmospheric conditions prevail especially during the winter, the main pollution season. When applied to other urban areas, the models can be expected to be more successful in areas where topography is less pronounced and where dispersion of atmospheric

In this thesis mathematical modelling of air pollution dispersion in urban areas has been inves gated. No substantial evidence has been found to suggest the existence of a uniquely applicable dispersion model. In general, the selection of the best applicable model is dictated by the nature of the specific problem, the availability of suitable experimental data and computing facilities. Such has been the case in the Pretoria study. On the basis of the research carried out, the often expressed notion that simple models cannot provide a satisfactory description of atmospheric pollution in urban areas must be rejected. On the contrary, the performance of the refined Gifford-Hanna simple model in the Pretoria urban area has been slightly better than the performance of the Gaussian plume model for multiple sources for two out of three time intervals examined. The simple models are, however, subject to large errors if applied indiscriminately to dispersion estimates under anomalous atmospheric conditions.

A substantial improvement on the immediate past usage of the Gifford-Hanna simple model has been made by developing seasonal, monthly and hourly equivalents of the original annual model. The ways in which this has been achieved had on purpose been chosen to be simple and inexpensive. The Gaussian plume model for multiple sources has likewise been refined by including horizontal wind and stability fields in the dispersion model. Once again, a simple interpolation scheme is used to derive the information from inexpensive meteorological observations. In addition to these contributions several aspects concerning air pollution modelling in a new area of application have been elucidated.

One of the main objectives of the thesis was to provide a basis for future urban air pollution modelling in South Africa. This has been done and two models of varying degrees of simplicity, the Gaussian plume model for multiple sources and the Gifford-Hanna simple model, have been evaluated, refined and verified using Pretoria as a model city. Owing to its valley situation the Pretoria area is effectively sheltered from outside interference by large-scale air movements and steady, well-defined atmospheric conditions prevail especially during the winter, the main pollution season. When applied to other urban areas, the models can be expected to be more successful in areas where topography is less pronounced and where dispersion of atmospheric

pollution is largely controlled by the diurnal and seasonal cycle of wind and stability regimes.

Sustained economic growth and a clean environment are equally required to ensure the well-being of an industrialized society. The present commitment to usage of coal and petroleum products as the dominant energy sources demands that economic policies are considered in conjunction with environmental concerns. A positive air pollution control policy, anticipatory in its nature, is needed to ensure continuing economic development and to prevent a significant infringement upon the quality of atmospheric environment. For an effective control and abatement of air pollution, it is necessary to relate key aspects of the control policy such as the placement of new emission sources and the required reduction of existing emissions with the production of pollutant concentration at points of social concern. Thus, a judicious use of air pollution dispersion models must be a central piece of any present or future air pollution strategy aiming at achieving a balance between growth and clean environment.

APPENDIX A

EXACT SOLUTIONS OF THE DIFFUSION EQUATION

The diffusion equation for concentration of particles in three dimensions has the form (Sutton, 1953)

$$\frac{d\chi}{dt} = \frac{\partial}{\partial x}\left(K_x \frac{\partial \chi}{\partial x}\right) + \frac{\partial}{\partial y}\left(K_y \frac{\partial \chi}{\partial y}\right) + \frac{\partial}{\partial z}\left(K_z \frac{\partial \chi}{\partial z}\right) \qquad (A.1)$$

where χ, K_x, K_y and K_z are space and time dependent variables. Analytical solutions of Equation (A.1) have been obtained for a number of special cases. In all the treatments Equation (A.1) is first reduced to the two-dimensional form

$$\frac{\partial \chi}{\partial t} + \bar{u}\frac{\partial \chi}{\partial x} + \bar{w}\frac{\partial \chi}{\partial z} = \frac{\partial}{\partial x}\left(K_x \frac{\partial \chi}{\partial x}\right) + \frac{\partial}{\partial z}\left(K_z \frac{\partial \chi}{\partial z}\right) \qquad (A.2)$$

where $\bar{u} = \left(\frac{\partial x}{\partial t}\right)$ and $\bar{w} = \left(\frac{\partial z}{\partial t}\right)$ are interpreted as the mean values of wind velocities along the x- and z- coordinates respectively. Physically, Equation (A.2) describes the dispersion of non-reactive matter released from an infinite crosswind line source. The special forms which have been adopted in order to obtain exact solutions of Equation (A.2) include

(i) the time dependence,
(ii) the functional form of the velocity variables $\bar{u}$ and $\bar{w}$,
(iii) the functional form of the eddy diffusivity K_z, and
(iv) the geometry of source.

In most investigations a steady-state conditions have been assumed thus removing the dependence of all variables on time. The summary of selected exact solutions of Equation (A.2) is presented in Table (A.1) for a line source geometry and in Table (A.2) for a point source geometry. Investigations in which the term $\left(\frac{\partial \chi}{\partial t}\right)$ has been retained for the solution of Equation (A.2) are marked in the column 1 of Tables (A.1) and (A.2) as time dependent. The time dependence concerns only the term $\left(\frac{\partial \chi}{\partial t}\right)$

providing a basis for the assessment of temporal variations in the concentration levels. The functional forms of the velocity variables and the eddy diffusivities are assumed to be time independent.

Table A.1. Summary of cases for which exact solutions exist for a line source geometry

Reference	Time dependent	Functional forms $\bar{u}$	$\bar{w}$	K_x	K_z
Roberts (1923)	Yes	0	0	K	K_v
		U	0	K	K_v
Calder (1949)		Uz^m	0	0	$K_v z^n$
Smith (1957)		$U(z+h)^a$	0	0	$K_v(z+h)^{1-a}$
Smith (1957)		U	W	0	$K_v(H-z)z$
Smith (1957)		U	W	0	$K_v z^{-a}$
Monin (1959)	Yes	0	0	0	$Kv_g z$
Walters (1969)		U	0	K-z	$K_v z$
Dilley and Yen (1971)		$(U-ax)(\frac{z}{z_1})^m$	$(\frac{az}{m+1})(\frac{z}{z_1})^m$	0	$K_v(\frac{z}{z_1})^n$
Calder (1971)		U_z^m	0	$K-z^\alpha$	$K_v z^\beta$

Table A.2. Summary of cases for which exact solutions exist for a point source geometry

Reference	Time dependent	Functional forms $\bar{u}$	$\bar{w}$	K_x	K_z
Roberts (1923)	Yes	0	0	K	K_v
Smith (1957)		$U(z+h)^{1/2}$	0	$K(z+h)^{1/2}$	$K_v(z+h)^{1/2}$
Yordanov (1965)		$U_1 z^m$	0	0	$K_1 z$
		U_2	0	0	$K_2 z^{4/3}$
Yordanov (1968)	Yes	0	0	0	$K_1 z^n$
	Yes	0	0	0	$K_1 (aL)^{n-(3/4)} z^{3/4}$
	Yes	0	0	0	$K_1 z^n$
	Yes	0	0	0	$K_1 (aL)^n$
Calder (1971)		U_z^m	0	$K-z^\alpha$	$K_v z^\beta$
Peters and Klinzing (1971)		U_z^m	0	0	Kx^n
Heines and Peters (1973)		$\bar{U}$	0	0	Kx^m
Lebedeff and Hameed (1976)		$\int \frac{u_g \Phi_m dz}{kz}$	0	0	$\frac{u_g kz}{\Phi_m}$

APPENDIX B

VERTICAL PROFILES OF WIND VELOCITY AND EDDY DIFFUSIVITY

The knowledge of vertical profiles of wind velocity and eddy diffusivity in the atmosphere is required in mathematical models of urban air pollution in which the gradient transport theory has been invoked to describe the process of dispersion.

B.1 Vertical profiles of wind velocity

Following the dimensional analysis of the main flow parameters in in the surface stress layer (Monin and Obukhov, 1954) the mean wind variation with height may be expressed as

$$\frac{d\bar{u}(z)}{dz} = \frac{1}{k}\,\frac{u_*}{z}\,\phi_m\left(\frac{z}{L}\right), \qquad (B.1)$$

where k is the von Karman constant and L is the Monin-Obukhov length. The parameter u_* is called the friction velocity and depicts the vertical variation of the shearing stress τ as

$$u_* = \sqrt{\left|\frac{\tau}{\rho}\right|} \qquad (B.2)$$

where ρ is the density of air. The friction velocity depends on the magnitude of the mean wind velocity, the atmospheric stability and the characteristics of the surface. Typical values of the ratio between the friction velocity and mean wind velocity at the anemometer height are listed in Table B.1.

It can be shown that the asymptotic solution of Equation (B.1) under near neutral atmospheric conditions assumes a logarithmic form

$$\bar{u}(z) = \frac{u_*}{k}\,\ln\left(\frac{z}{z_o}\right) \qquad (B.3)$$

The surface roughness length z_o represents the aerodynamical roughness of the surface. Typical values of the surface roughness length are listed in Table B.1.

Table B.1. Typical values of the surface roughness length z_o and the ratio (u_*/u) (after Pasquill, 1974)

Thermal stratification Wind speed (m/sec)		Neutral 10	Unstable 5	 2
z_o (cm)	Surface	Ratio (u_*/u)		
0,1	Very closely mown grass	0,04	0,05	0,07
1	Short grass	0,06	0,07	0,09
3	Long grass	0,07	0,08	0,10
20	Rural-agricultural complex	0,10	0,11	0,15
100	Forests, urban areas	0,17	0,18	0,23

Thermal stratification of the atmosphere causes considerable departures from the logarithmic profile and the universal function ϕ_m in Equation (B.1) must be evaluated for various stability conditions. When the function ϕ_m is expanded in Taylor series and only the first two terms

$$\phi_m\left(\frac{z}{L}\right) = 1+\alpha\,\frac{z}{L} \tag{B.4}$$

are retained, a log-linear profile

$$\bar{u}(z) = \frac{u_*}{k}\left[\ln\left(\frac{z}{z_o}\right) + \alpha\frac{z}{L}\right] \tag{B.5}$$

is obtained by integrating Equation (B.1). The value of the parameter α in Equation (B.5) has to be determined experimentally. Webb (1970) has proposed the value of $\alpha = 5,2$ for stable conditions and $\alpha = 4,5$ for unstable conditions. Businger (1966) has suggested $\alpha = 4,7$ for stable conditions and the use of an alternative form of

the function ϕ_m for unstable conditions as

$$\phi_m\left(\frac{z}{L}\right) = \left(1 - 15\,\frac{z}{L}\right)^{-\frac{1}{4}} \qquad (B.6)$$

Several interpolation formulae have been suggested to describe the variation of wind speed with height above the surface stress layer. Blackadar (1962) has modified the log-linear profile derived for the surface stress layer by including the effect of the Coriolis force. The profile is given as

$$\bar{u}\,(z) = \frac{u_{*o}}{k}\,\ln\left(\frac{z}{z_o}\right) + 144\,fz \qquad (B.7)$$

where the symbol u_{*o} refers to friction velocity calculated at the surface and f is the Coriolis parameter. Some of the alternative expressions are shown in Table B.2.

F. Vertical profiles of eddy diffusivity

The simplest form describing the vertical profile of the eddy diffusivity K_z is consistent with the power law for the variation of wind velocity with height. If K_1 is a known value of K_z at a height z_1, the power law may be written, following Sutton (1953) as

$$\frac{K_z\,(z)}{K_1} = \left(\frac{z}{z_1}\right)^n \qquad (B.8)$$

The parameter n may be determined experimentally or from the available information on wind profile by the application of the conjugate law

$$n = 1 - m \qquad (B.9)$$

The available experimental evidence (Cohen et.al., 1972, Ikebe and Shimo, 1972) indicates a close range of values from n = 1,2 to 1,5.

In some dispersion models more complex forms of K_z have been used. It follows from the similarity arguments that K_z is linearly proportional to the height z under neutral conditions

Table B.2. Functional forms of wind and eddy diffusivity profiles (after Ragland and Pierce, 1975)

Stability	Maximum range	Wind profile	Eddy diffusivity profile
	$z_{(max)}$	u(z)	K(z)
		Surface stress layer	
Neutral	400 u_*	$\frac{u_*}{0,4} \ln\left(\frac{z+z_o}{z_o}\right)$	$0,4\ u_* z$
	L	$\frac{u_*}{0,4}\left[\ln\left(\frac{z+z_o}{z_o}\right) + \frac{5,2z}{L}\right]$	$0,4\ u_* z\ /\ (1+\frac{5,2}{L} z)$
Stable	6L	$\frac{u_*}{0,4}\left[\ln\left(\frac{z+z_o}{z_o}\right) + 5,2\right]$	$0,4\ u_* z\ /\ 6,2$
Unstable	2L	$\frac{u_*}{0,4}\left[2(\tan^{-1}\phi - \tan^{-1}\phi_o + \ln(\frac{\phi-1}{\phi_o-1}) - \ln(\frac{\phi+1}{\phi_o+1})\right]$	$0,4\ u_* z\ (1 - \frac{15z}{L})^{0,25}$
		Above surface stress layer	
Neutral	z_m	$(u_g - u)\left(\frac{z - 400u_*}{z_m - 400u_*}\right)^{0,2} + u$	$0,4\ u_* (400u_*)$
Stable	z_m	$(u_g - u)\left(\frac{z - 6L}{z_m - 6L}\right)^{0,5} + u$	$0,4\ u_* L$
Unstable	z_m	$(u_g - u)\left(\frac{z + 2L}{z_m + 2L}\right)^{0,2} + u$	$0,4\ u_* (400u_*)\left(1 - \frac{6000u_*}{L}\right)^{0,25}$

Notation: U_g denotes the speed of the geostrophic wind, u is the wind speed in the surface stress layer and the symbols ϕ and ϕ_0 are defined as $\phi = \left[1 - 15\ (z + z_o)\ /L\right]^{0,25}$; $\phi_o = (1 - 15z_o/L)^{0,25}$.

$$K_z(z) = ku_* z \tag{B.10}$$

If diabatic conditions prevail, the universal function ϕ_m is used to modify the K_z profile (Monin and Obukhov, 1954) as

$$K_z(z) = \frac{ku_* z}{\phi_m\left(\frac{z}{L}\right)} \tag{B.11}$$

[illegible]ional forms of the eddy diffusivity p[illegible]iles have been summarized in Table B.2.

Several workers (Randerson, 1970, Mahoney and Egan, 1970, Shir and Shieh, 1974, Ragland and Pierce, 1975, Bankoff and Hanzevack, 1975) have proposed approximate profiles of K_z for use in urban dispersion models. The profiles are summarized in Table B.3 together with the corresponding wind profile and the type of the emission source. In order to account for the modification of the eddy diffusivity in urban areas Liu and Durran (1977) have adopted a technique developed by O'Brien (1970) to calculate the vertical eddy diffusivity as a function of the surface roughness length. Using a simple relationship between the vertical eddy diffusivity K_z and the Gaussian variance of plume distribution σ_z

$$K_z = \frac{1}{2}\left(\frac{d\sigma_z^2}{dt}\right) \tag{B.12}$$

they have found a good agreement between the calculated values of K_z for z_o = 50 cm and observed values of σ_z for urban areas as reported by McElroy and Pooler (1968).

Table 3.3. Simplified forms of eddy diffusivity and wind profiles adopted in some urban air pollution dispersion models

Model	Eddy diffusivity profile K(z)	Wind profile u(z)	Type of source
Randerson (1970)	$\left[K(10)\ A\ \frac{z}{1\,000}\ \left(1 - \frac{z}{1\,000}\right)^{m}\right]$	$\frac{u_*}{k} \ln\left(\frac{z-d}{z_o}\right)$	point
Mahoney and Egan (1970)	$0{,}16z$ for $0 < z < 100$ m $\left[16 - 0{,}32\ (z-150)\right]$ for $100 < z < 150$ m $150 < z < 200$ m	$\frac{z}{k} \ln\left(\frac{z+z_o}{z_o}\right)$	line
Shir and Shieh (1974)	$u_* k z e^{-\left(\frac{4z}{h\phi}\right)}$	$u_o \left(\frac{z}{z_o}\right)^{p}$	point
Ragland and Pierce (1975)	$k u_* z$	$\frac{u_*}{k} \ln\left(\frac{z+z_o}{z_o}\right)$	line
Bankoff and Hanzevack (1975)	constant	$u_o \left(\frac{z}{z_o}\right)^{p}$	point

APPENDIX C

AN EXAMPLE OF THE WIND DATA FOR JULY 1977 IN PRETORIA

All wind speeds are given in kilometres per hour.

SURFACE WINDS — PRETORIA — SHOWGROUNDS Site No.2 — JULY 1977

DATE/HOURS	1	2	3	4	5	6	7	8	9	10	11	12	13	14	15	16	17	18	19	20	21	22	23	24
1 7 77	E 7	SW 6	W 7	WSW 6	SSW 3	ESE 4	SE 9	SE 16	SE 16	S 15	SE 18	SE 16	E 14	E 14	E 15	SE 12	E 12	ESE 11	SE 14	ESE 24	ESE 27	ESE 28	ESE 32	ESE 32
2 7 77	ESE 31	E 27	ESE 25	ESE 24	ESE 20	ESE 23	SE 17	ESE 17	ESE 21	ESE 23	ESE 17	E 14	ENE 12	NE 12	E 10	E 11	NE 7	ENE 6	ESE 4	ESE 4	ESE 9	ESE 19	ESE 20	ESE 11
3 7 77	ESE 14	ESE 15	E 19	ESE 15	ESE 8	SE 7	SSE 4	S 3	ENE 2	E 2	NE 5	ENE 7	E 7	ESE 9	E 9	E 8	ESE 7	E 5	SE 5	NW 1	ESE 4	SE 2	WSW 2	ENE 2
4 7 77	E 1	E 2	E 3	W 2	W 3	SSW 1	E 1	WNW 3	NNW 2	NNW 2	NW 5	WNW 10	WNW 9	WNW 9	NW 8	WSW 7	NW 5	WNW 8	WSW 5	SW 3	SSE 2	WSW 2	WNW 2	S 2
5 7 77	E 5	SW 3	E 4	SSW 2	ENE 1	WNW 1	W 1	W 5	NNE 2	NNW 2	WNW 3	WNW 10	WNW 9	NW 10	NNW 12	NW 10	NNE 10	NNE 3	NNE 6	NNW 3	NW 1	NNW 1	NNW 2	NNW 1
6 7 77	WNW 1	NNW 3	NNW 2	NNW 1	NNW 1	NNW 1	NNW 1	NNW 1	NNW 1	NNW 1	NNW 5	WNW 11	WNW 20	W 23	WSW 21	W 28	SW 24	SSW 20	SSW 29	SSW 28	S 23	S 26	SSE 14	SSE 10
7 7 77	SE 7	S 6	SSW 8	S 7	W 5	SSE 12	SSE 6	SSE 9	E 13	ESE 23	E 21	ENE 17	NE 20	NNE 15	NE 14	NNE 13	N 13	NNE 10	ENE 8	E 1	ESE 4	E 4	ESE 5	SE 2
8 7 77	ESE 4	ESE 5	ESE 4	SE 2	ESE 3	SE 1	WNW 1	CAL 0	NNW 2	N 3	NW 6	WNW 10	NW 9	W 7	W 7	WNW 7	WNW 4	WNW 7	W 7	WSW 7	E 2	ESE 2	WSW 2	WNW 1
9 7 77	NW 1	NNW 1	WNW 1	W 1	W 4	SW 2	WSW 3	WNW 4	W 4	WNW 3	NW 3	SE 3	NNW 7	NNE 7	E 6	S 1	S 13	S 13	SSE 19	SSE 24	SSE 24	SSE 12	S	S 5
10 7 77	S 3	S 2	SSE 5	SSE 5	S 5	SE 4	SE 4	SE 1	W 1	ENE 2	NE 12	NE 16	NNE 19	N 20	NNE 19	NE 14	NE 17	NE 13	ENE 11	ENE 11	NE 14	NE 21	NE 15	NE 13
11 7 77	ENE 10	ENE 9	ENE 7	E 6	E 4	E 6	ESE 6	E 4	ENE 5	NE 6	NNW 3	WSW 4	WNW 11	WNW 11	WNW 14	WNW 13	WNW 15	WNW 10	WNW 7	WNW 3	WSW 2	ESE 1	SSE 2	NW 2	SE 4
12 7 77	WSW 3	W 4	WSW 2	E 2	E 2	NE 2	W 1	WNW 5	NNW 2	WNW 3	SW 12	SW 10	SW 10	SW 9	WSW 9	SSW 8	SW 7	SSW 8	S 11	SSE 6	SSE 6	SE 4	SSW 5	SSE 4
13 7 77	E 4	ESE 2	ESE 3	SSW 2	SE 2	ESE 7	E 7	ESE 7	ENE 8	ENE 10	NE 7	NW 7	WNW 10	WNW 10	W 12	SW 10	WNW 6	WNW 7	WSW 5	WSW 7	SW 1	SSE 1	W 4	S 2
14 7 77	S 2	WNW 3	S 9	SSE 7	SSE 7	SSW 5	S 5	S 5	SSE 7	E 5	NNE 6	E 6	NE 8	NE 8	NNE 15	NE 11	NNE 17	NNE 11	NE 10	NE 9	NE 9	NE 11	ESE 11	E 9
15 7 77	E 9	E 11	ESE 12	E 9	E 4	NE 5	E 3	E 1	NNE 1	NE 7	NE 8	NW 7	ESE 5	WNW 7	ENE 7	NW 6	NNW 6	NW 3	SSW 2	NE 5	ESE 6	SE 4	SE 1	WSW 2
16 7 77	ENE 2	NNW 1	WNW 4	NE 1	WSW 2	ENE 2	SSE 1	W 1	NNE 1	NNW 2	NNE 4	NE 5	ENE 7	ENE [illegible]	NE [illegible]	[illegible]	[illegible]	N 7	N 5	NE 4	E 4	ESE 4	E 2	ENE 8
17 7 77	E 7	E 7	ESE 7	ESE 4	E 1	E 2	ESE 1	ESE 1	NNE 2	N 4	NW 10	NW 14	W 15	W 17	W 1[illegible]	[illegible] 16	WNW 10	WNW 9	W 9	N 3	W 4	SW 3	WSW 3	W 5
18 7 77	W 2	CAL 0	WSW 3	NE 3	WNW 2	SSE 6	SSE 5	SE 4	ENE 4	E 4	ENE 3	WNW 5	WNW 5	S 8	N 10	[illegible]	[illegible]	NW 6	WNW 8	WSW 7	SSW 2	S[illegible] 2	E 2	WSW 3	SE 7

| | | |

FREQUENCIES FOR HOURS 6.00 - 9.00

WIND SPEED	WIND DIRECTION																	TOTAL
	N	NNE	NE	ENE	E	ESE	SE	SSE	S	SSW	SW	WSW	W	WNW	NW	NNW	CAL	VAR	
0- 4	1	5	5	5	7	2	3	3	3	1	1	3	11	7	4	6	1	0	68
5- 8	0	0	0	2	1	2	0	2	2	1	0	0	1	1	0	0	0	0	11
9-16	0	0	0	0	1	2	1	0	0	0	0	0	0	0	0	0	0	0	4
17-30	0	0	3	0	0	0	0	0	0	0	0	0	0	0	0	0	0	0	0
>30	0	0	0	0	0	0	0	0	0	0	0	0	0	0	0	0	0	0	0
TOTAL	1	5	8	7	9	6	7	6	7	2	1	3	12	8	4	6	1	0	93
%TOTAL	1.1	5.4	5.6	7.5	9.7	6.5	7.5	6.5	7.5	2.2	1.1	3.2	12.9	8.6	4.3	6.5	1.1	0.0	100.0%

FREQUENCIES FOR HOURS 9.00 - 12.00

WIND SPEED	WIND DIRECTION																	TOTAL
	N	NNE	NE	ENE	E	ESE	SE	SSE	S	SSW	SW	WSW	W	WNW	NW	NNW	CAL	VAR	
0- 4	2	2	1	2	1	0	1	0	0	0	0	1	0	3	2	6	0	0	21
5- 8	3	3	3	1	2	0	1	0	0	0	0	0	0	3	6	4	0	0	31
9-16	0	1	4	1	1	1	2	0	2	2	0	0	0	5	2	1	0	0	27
17-30	0	1	2	1	1	3	1	0	0	0	0	0	1	5	0	0	0	0	14
>30	0	0	0	0	0	0	0	0	0	0	0	0	0	0	0	0	0	0	0
TOTAL	5	7	10	5	5	4	5	0	2	2	0	1	1	16	10	11	0	0	93
%TOTAL	5.4	7.5	10.8	5.4	5.4	4.3	5.4	0.0	2.2	2.2	0.0	1.1	1.1	17.2	10.8	11.8	0.0	0.0	100.0%

FREQUENCIES FOR HOURS 12.00 - 15.00

WIND SPEED	WIND DIRECTION																	TOTAL
	N	NNE	NE	ENE	E	ESE	SE	SSE	S	SSW	SW	WSW	W	WNW	NW	NNW	CAL	VAR	
0- 4	0	0	0	0	0	0	0	0	0	0	0	0	0	0	1	0	0	0	1
5- 8	0	2	3	2	2	1	0	0	1	2	3	1	4	11	5	3	0	0	29
9-16	1	3	4	4	4	1	0	0	0	0	0	1	2	4	2	2	0	0	28
17-30	1	2	1	0	0	0	0	0	0	0	0	0	0	0	0	0	0	0	4
>30	0	0	0	0	0	0	0	0	0	0	0	0	0	0	0	0	0	0	0
TOTAL	2	7	8	6	6	2	0	0	1	2	3	2	6	15	8	5	0	0	93
%TOTAL	2.2	7.5	8.6	6.5	6.6	2.2	0.0	0.0	1.1	2.2	3.2	2.2	6.5	16.1	8.6	5.4	0.0	0.0	100.0%

FREQUENCIES FOR HOURS 15.00 - 18.00

WIND SPEED	WIND DIRECTION																	TOTAL
	N	NNE	NE	ENE	E	ESE	SE	SSE	S	SSW	SW	WSW	W	WNW	NW	NNW	CAL	VAR	
0- 4	0	1	0	0	0	0	0	1	1	1	0	0	0	0	1	1	0	0	6
5- 8	3	1	1	2	2	1	0	1	0	1	2	1	0	9	5	6	0	0	38
9-16	2	7	3	0	2	1	1	0	2	0	1	0	1	10	4	3	0	0	41
17-30	0	0	1	0	0	0	0	0	0	0	0	0	3	3	0	1	0	0	8
>30	0	0	0	0	0	0	0	0	0	0	0	0	0	0	0	0	0	0	0
TOTAL	5	9	5	2	4	2	1	2	3	2	3	1	4	22	10	11	0	0	93
%TOTAL	5.4	9.7	5.4	2.2	4.3	2.2	1.1	2.2	3.2	2.2	3.2	1.1	4.3	23.7	10.8	11.8	0.0	0.0	100.0%

FREQUENCIES FOR HOURS 18.00 - 21.00

WIND SPEED	WIND DIRECTION																			
	N	NNE	NE	ENE	E	ESE	SE	SSE	S	SSW	SW	WSW	W	WNW	NW	NNW	CAL	VAR	*	TOTAL
0- 4	0	0	2	2	4	4	4	2	0	2	3	2	5	1	3	4	0	0	*	34
5- 8	1	1	1	1	1	2	3	3	1	0	0	10	4	2	0	0	0	0	*	30
9-16	0	0	5	2	0	0	1	1	1	2	0	0	7	0	0	0	0	0	*	17
17-30	0	0	0	0	0	2	0	0	0	0	0	0	0	0	0	0	0	0	*	8
>30	0	0	0	0	0	0	0	0	0	0	0	0	0	0	0	0	0	0	*	0
TOTAL	1	1	8	5	5	8	8	6	2	4	3	12	16	3	3	4	0	0	*	93
%TOTAL	1.1	1.1	8.6	5.4	5.4	8.6	8.6	9.7	3.2	4.3	3.2	12.9	17.2	3.2	3.2	4.3	0.0	0.0	*	100.0%

FREQUENCIES FOR HOURS 21.00 - 24.00

WIND SPEED	WIND DIRECTION																			
	N	NNE	NE	ENE	E	ESE	SE	SSE	S	SSW	SW	WSW	W	WNW	NW	NNW	CAL	VAR	*	TOTAL
0- 4	0	1	0	2	3	2	6	3	3	2	2	8	7	1	3	6	1	0	*	57
5- 8	0	0	0	3	0	1	3	0	1	1	0	1	5	0	0	0	0	0	*	14
9-16	0	0	0	2	3	3	2	3	0	0	0	1	1	0	0	0	0	0	*	15
17-30	0	0	1	0	0	0	1	0	1	0	0	0	0	0	0	0	0	0	*	5
>30	0	0	0	0	0	0	2	0	0	0	0	0	0	0	0	0	0	0	*	2
TOTAL	0	1	1	7	6	6	15	6	5	3	2	10	13	1	3	6	1	0	*	93
%TOTAL	0.0	1.1	1.1	7.5	6.5	6.5	16.1	6.5	5.4	3.2	2.2	10.8	14.0	1.1	3.2	6.5	1.1	0.0	*	100.0%

FREQUENCIES FOR HOURS 0.00 - 24.00

WIND SPEED	WIND DIRECTION																			
	N	NNE	NE	ENE	E	ESE	SE	SSE	S	SSW	SW	WSW	W	WNW	NW	NNW	CAL	VAR	*	TOTAL
0- 4	3	9	11	17	31	27	21	15	13	10	8	23	40	19	18	37	4	0	*	306
5- 8	7	7	13	11	13	17	11	11	3	7	3	13	22	20	16	13	0	0	*	192
9-16	3	11	19	15	19	9	7	7	12	6	8	2	17	16	9	6	0	0	*	175
17-30	1	3	9	1	4	14	2	3	3	6	1	1	3	14	2	1	0	0	*	68
>30	0	0	0	0	0	3	0	0	0	0	0	0	0	0	0	0	0	0	*	3
TOTAL	14	30	52	44	66	70	41	36	36	29	20	39	82	79	45	57	4	0	*	744
%TOTAL	1.9	4.0	7.0	5.9	8.9	9.4	5.5	4.8	4.8	3.9	2.7	5.2	11.0	10.6	6.0	7.7	0.5	0.0	*	100.0%

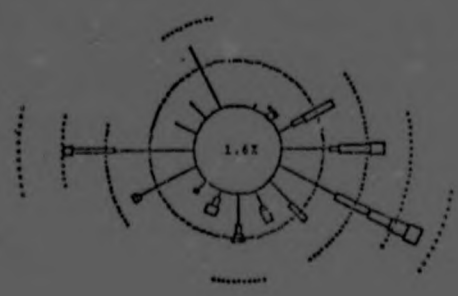
NO. OF ENTRIES FOR THIS MONTH: 744

DAILY AVERAGES (KM/H):
15 , 16 , 7 , 4 , 5 , 12 , 10 , 4 , 7 , 10 , 7 , 6 , 6 , 8 , 5 , 5 , 8 , 5 , 7 , 4 , 4 , 3 , 6 , 5 , 8 , 8 , 5 , 5 ,
12 , 14 , 11 ,

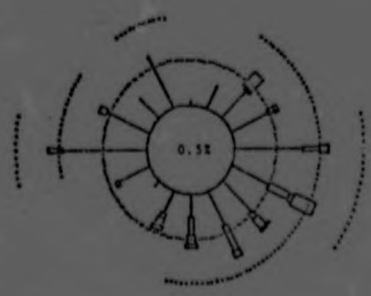
HOURLY AVERAGES (KM/H):
4 , 4 , 4 , 5 , 4 , 5 , 4 , 5 , 5 , 7 , 10 , 11 , 12 , 12 , 12 , 11 , 11 , 9 , 8 , 7 , 6 , 6 , 6 , 6 ,

AVERAGE WIND SPEED FOR THIS MONTH (KM/H): 8

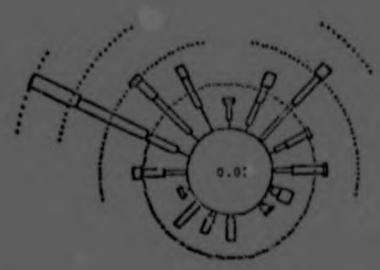
SURFACE WINDS PRETORIA SHOWGROUNDS Site No.2 JULY 1977



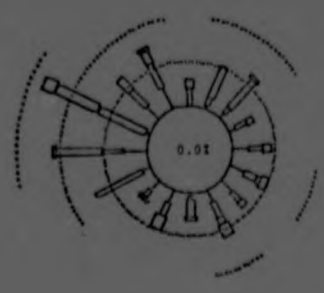
FREQUENCIES FOR HOURS
21.00 - 3.00



FREQUENCIES FOR HOURS
3.00 - 9.00

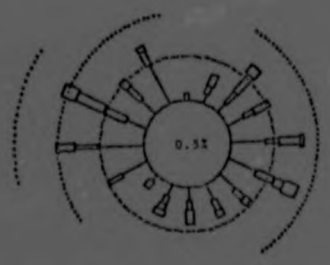


FREQUENCIES FOR HOURS
9.00 - 15.00



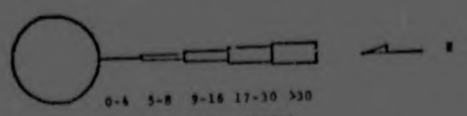
FREQUENCIES FOR HOURS
15.00 - 21.00

1



FREQUENCIES FOR HOURS
0.00 - 24.00

KEY TO WINDROSES



0-4 5-8 9-18 17-30 >30
WIND SPEED (KM/H)

ARCS REPRESENT 5% FREQUENCY INTERVALS

REFERENCES

Bankoff, S.G., and Hanzevack, E.L. (1975) The adaptive-filtering transport model for prediction and control of pollutant concentration in an urban airshed. Atmos. Environ., 9:793-808.

Barth D.S. (1970) Federal motor vehicle emission goals for CO, HC and NO based on desired air quality levels. J. Air Poll. Control Assoc., 20:519-523.

Batchelor, G.K. (1950) The application of the similarity theory of turbulence to atmospheric diffusion. Quart. J. R. Met. Soc., 76:133-146.

_____ (1964) Diffusion from sources in a turbulent boundary layer. Archiv Mechaniki Stosowanej, 3:661-670.

Beran, D.W., Hall, F.F., Wescott, J.W., and Neff, W.D. (1971) Application of an acoustic sounder to air pollution monitoring. Symposium on Air Poll., Turbulence and Diffusion. Amer. Met. Soc., Las Cruces, New Mexico: 66-72.

Blackadar, A.K. (1962) The vertical distribution of wind and turbulent exchange in a neutral atmosphere. J. Geophys. Res., 67:3095-3102.

Bornstein R.D. (1968) Observations of the urban heat island effect in New York City. J. Appl. Met., 7:575-582.

Briggs, G.A. (1969) Plume Rise. U.S. Atomic Energy Commission Publication TID-25075: 82pp.

_____ (1974) Diffusion estimation for small emissions. NOAA, ATDL Report 106. Oak Ridge, Tennessee: 62pp.

Brooks, C.E.P., and Carruthers, N. (1953) Handbook of Statistical Methods in Meteorology. Meteorological Office, London: 412pp.

Bruntz, S.M., Cleveland, W.S., Kleiner, B., and Warner, J.L. (1974) The dependence of ambient ozone on solar radiation, wind, temperature and mixing height. Proc. of Symposium on Atmospheric Turbulence and Diffusion. Amer. Met. Soc., Santa Barbara, California: 125-128.

Busch, N.E. (1973) On the mechanics of atmospheric turbulence. Workshop on Micrometeorology, D.A. Haugen (ed.). Amer. Met. Soc., Boston: 1-65.

Businger, J.A. (1966) Transfer of momentum and heat in the planetary boundary layer. Proc. of Symposium on Arctic Heat Budget and Atmospheric Circulation. The Rand Corporation, Santa Monica, California: 305-332.

Busse, A.D., and Zimmerman, J.R. (1973) User's guide for the climatological dispersion model. EPA Publication PB-227-346. Research Triangle Park, N. Carolina: 131pp.

Calder, K.L. (1949) Eddy diffusion and evaporation in flow over aerodynamically smooth and rough surfaces. Quart. J. Mech. Appl. Math., 2:153-176.

_____ (1971) Some applications of generalized similarity analysis to the theory of atmospheric diffusion and evaporation. Symposium on Air Poll., Turbulence and Diffusion. Amer. Met. Soc., Las Cruces, New Mexico.

Carpenter, S.B., Montgomery, T.L., Leavitt, J.M., Colbaugh, W.C., and Thomas, F.W. (1971) Principal plume dispersion models: TVA power plants. J. Air Poll. Control Assoc., 21:491-495.

Chandrasekhar, S. (1961) Hydrodynamic and Hydromagnetic Stability. Oxford University Press, London: 652pp.

Clarke, J.F. (1964) A simple diffusion model for calculating point concentrations from multiple sources. J. Air Poll. Control Assoc., 14:347-352.

Cohen, L.D., Barr, S., Krablin, R., and Newstein, H. (1972) Steady-state vertical turbulent diffusion of radon. J. Geophys. Res., 77:2654.

Crawford, K.C., and Hudson, H.R. (1970) Behaviour of winds in the lowest 1 500 feet in central Oklahoma, June 1966 - May 1967. ESSA Technical Memorandum ERLRM-NSSL, U.S. Department of Commerce, Norman, Oklahoma: 48pp.

Davidson, B. (1967) A summary of the New York urban air pollution dynamics research program. J. Air Poll. Control Assoc., 17:154-158.

Deardorff, J.W. (1972) Numerical investigation of neutral and unstable planetary boundary layers. J. Atmos. Sci., 29:91-115.

_____ (1973) Three-dimensional numerical modelling of the planetary boundary layer. Workshop on Micrometeorology, D.A. Haugen (ed.). Amer. Met. Soc., Boston:271-311.

De Marrais, G.A. (1959) Wind speed profiles at Brookhaven National Laboratory. J. Appl. Met., 16:181.

_____ (1961a) Vertical temperature differences observed over an urban area. Bull. Amer. Met. Soc., 42:548-554.

_____ (1961b) Meteorology for land development planning in the Tulsa metropolitan area. Technical Report A61 - 5, U.S. Department of Health, Education and Welfare, Cincinnati, Ohio: 28pp.

Demerjian, K.L., Kerr, J.A., and Calvert, J.G. (1974) The mechanism of photochemical smog formation. Advances in Environ. Sci. Tech., 4, J.A. Pitts and R.L. Metcalf (eds.). Wiley, New York: 382pp.

De Nevers, N., and Morris, J.R. (1975) Rollback modelling-basic and modified. J. Air Poll. Control Assoc., 25:943-947.

Dickerson, M.H. (1975) A three-dimensional mass-consistent atmospheric flux model for regions with complex topography. Paper presented at the First Conference on Regional and Mesoscale Modelling, Analysis and Prediction. Las Vegas, Nevada, May 6-9.

Dilley, J.F., and Yen, K.T. (1971) Effect of a mesoscale type wind on the pollutant distribut... from a line source. Atmos. Environ., 11:312-322.

Donaldson, C. du P. (1973) Construction of a dynamic model of the production of atmospheric turbulence and the dispersal of atmospheric pollutants. Workshop on Micrometeorology, D.A. Haugen (ed.). Amer. Met. Soc., Boston:313-392.

Donaldson, C. du P., and Hilst, G.R. (1972) Effect of inhomogeneous mixing on atmospheric photochemical reactions. Environ. Sci. and Tech., 6:812-816.

DSIR (1945) Atmospheric pollution in Leicester. A scientific survey. Technical Paper No. 1, London: 161pp.

Duckworth, F.S., and Sandberg, J.S. (1954) The effect of cities upon horizontal and vertical temperature gradients. Bull. Am. Met. Soc., 35:198-207.

Egan, B.A. (1975) Turbulent diffusion in complex terrain. Lectures on Air Poll. and Environ. Impact Analysis, D.A. Haugen (ed.). Amer. Met. Soc., Boston:112-135.

Eliassen, A., and Saltbones, J. (1975) Decay and transformation rates of SO_2, as estimated from emission data, trajectories and measured air concentrations. Atmos. Environ., 9:425-429.

Eschenroeder, A.Q., and Martinez, J.R. (1973) Concepts and applications of photochemical smog models. Adv. in Chem. Ser., 113.

Estoque, M.A. (1973) Numerical modelling of the planetary boundary layer. Workshop on Micrometeorology, D.A. Haugen (ed.). Amer. Met. Soc., Boston:217-270.

Fortak, H.G. (1970) Numerical simulation of temporal and spatial distribution of urban pollution concentration. Proc. of Symposium on Multiple Source Urban Diff. Models. U.S. EPA Publ. No. AP-86, Chapel Hill, N. Carolina: 9.1-9.34.

Frenkiel, F.N. (1956) Atmospheric pollution and zoning in an urban area. The Scientific Monthly: 194-203.

Friedlander, S.K., and Seinfeld, J.H. (1969) A dynamic model of photochemical smog. Environ. Res. and Tech., 3:1175-1180.

Garstang, M. (1977) Surface structure of convective rain. Final report to the Atmospheric Science Section, National Science Foundation. Washington, D.C: 94pp.

Giebel, J. (1977) Untersuchungen zur Abbaurate von Schwefeldioxid in der Atmosphäre. Schriftreihe der Landesanstalt für Immissionsschutz des Landes Nordrhein - Westfalen. Heft 40, Essen 22.

Gifford, F.A. (1959) Computation of pollution from several sources. J. Air Poll. Control Assoc., 2:109-110.

Author Zib P
Name of thesis Modelling the dispersion of airborne Pollutants in the Pretoria urban Area 01158

PUBLISHER:
University of the Witwatersrand, Johannesburg
©2013

LEGAL NOTICES:

Copyright Notice: All materials on the University of the Witwatersrand, Johannesburg Library website are protected by South African copyright law and may not be distributed, transmitted, displayed, or otherwise published in any format, without the prior written permission of the copyright owner.

Disclaimer and Terms of Use: Provided that you maintain all copyright and other notices contained therein, you may download material (one machine readable copy and one print copy per page) for your personal and/or educational non-commercial use only.

The University of the Witwatersrand, Johannesburg, is not responsible for any errors or omissions and excludes any and all liability for any errors in or omissions from the information on the Library website.